REPORT DOCUMENTATION PAGE

Form Approved
OMB No. 0704-0188

1. AGENCY USE ONLY *(Leave Blank)*	2. REPORT DATE	3. REPORT TYPE AND DATES COVERED
	December 1995	Final Technical Report 04/15/94-10/15/95

4. TITLE AND SUBTITLE

Halogen Azide Visible Chemical Laser

5. FUNDING NUMBERS

F49620-94-C-0025
63218C
1601/08
AFOSR-TR-960011

6. AUTHOR(S)

D.J. Benard and E. Boehmer

7. PERFORMING ORGANIZATION NAME(S) AND ADDRESS(ES)

Rockwell Science Center
P.O. Box 1085
Thousand Oaks, CA 91358

8. PERFORMING ORGANIZATION REPORT NUMBER

SC71099.FTR

9. SPONSORING / MONITORING AGENCY NAME(S) AND ADDRESS(ES)

Air Force Office of Scientific Research/NE NL
Directorate of Chemistry and Material Sciences
110 Duncan Avenue, Suite B-115
Bolling AFB, DC 20332-001
Dr Berman

10. SPONSORING / MONITORING AGENCY REPORT NUMBER

19960207 024

11. SUPPLEMENTARY NOTES

12a. DISTRIBUTING/AVAILABILITY STATEMENT

Approved for public release;
Distribution Unlimited

12b. DISTRIBUTION CODE

DISTRIBUTION STATEMENT A
Approved for public release;
Distribution Unlimited

13. ABSTRACT *(Maximum 200 Words)*

Previous work established two visible wavelength chemical lasers based on production of metastable NF from fast thermal dissociation of FN3, and energy transfer from NF* to either BiF or BH. These lasers were inefficient, due to donors which yielded low concentrations of emitting molecules. The present work focused on improvements in emitter scaling to achieve higher efficiency in these laser systems. Pentaborane was found to generate BH comparable to diborane, and dimethyldiazidodiborane was synthesized and shown to be a superior BH source, although additional improvements are still required. Modeling of precombustion systems to improve the NF/BiF laser demonstrated that TMB dissociates rapidly at 3500 K but CH3 byproducts fail to recombine. The rate of NF* quenching by CH3 radicals was measured and found to be 9.2E-11 cm3/s. The precombustion systems, H2 + F2, H2 + NF3, N20 + CO and C2N2 + O2 were examined for use as chemical processors of TMB to improve the yield of BiF. The F2 system was unstable with TMB, the NF3 system generated products that spontaneously react FN3, the C2N2 system favored Bi-atoms over BiF, and the N2O system enhanced the yield of BiF but also generated byproducts that optically absorb at the laser wavelength. Finally, energy transfer from metastable NF to iodine was examined, since scalable I-atom production was less problematical in this system. Unfortunately, while the transfer reaction was both fast and efficient, fast NF induced E-V quenching of the excited I-atoms prevented attainment of a population inversion.

14. SUBJECT TERMS

High energy chemical laser, visible wavelength, fluorine azide, metastable NF, energy transfer, energy pooling, bismuth fluoride, boron hydride, advanced donors, iodine, kinetics, dissociation, quenching, power extraction efficiency

15. NUMBER OF PAGES

53

16. PRICE CODE

17. SECURITY CLASSIFICATION OF REPORT	18. SECURITY CLASSIFICATION OF THIS PAGE	19. SECURITY CLASSIFICATION OF ABSTRACT	20. LIMITATION OF ABSTRACT
UNCLASSIFIED	UNCLASSIFIED	UNCLASSIFIED	UL

SC71099.FTR

Halogen Azide Visible Chemical Laser

Final Technical Report
April 15, 1994 through October 15, 1995
Contract No. F49620-94-C-0025

Prepared for:
Maj. Glen Perram
Air Force Office of Scientific Research
Directorate of Chemical and Atmospheric Sciences
Bolling AFB, DC 20332

Prepared by:
D. Benard and E. Boehmer
Rockwell Science Center
1049 Camino Dos Rios
Thousand Oaks, CA 91360

December 1995

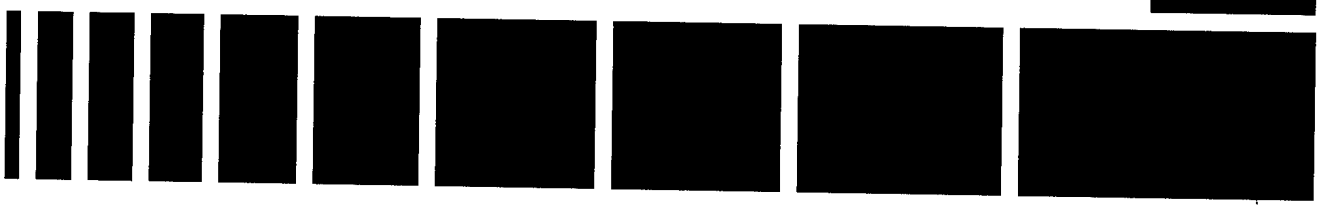

Rockwell

Science Center

Copy # 2

Table of Contents

Background

The object of this work was to develop an efficient chemical gain medium suitable for visible wavelength high energy laser applications. Achieving this goal requires:

1. Demonstrating an efficient and scalable chemical source of electronically excited metastable atoms or molecules.

2. Identifying a transfer agent that will rapidly accept energy from the metastables to generate a population inversion on a transition at visible wavelength.

3. Developing a source of the emitting molecules capable of operating at densities adequate to extract the metastable energy before it decays by other means.

Under prior contracts, the first two of these goals have already been met. Fast thermal dissociation of FN_3 was shown to yield up to 3 x $10^{16}/cm^3$ densities of metastable NF($a^1\Delta$) with near unit quantum efficiency.[1] At this density, the power flux in supersonic flow approaches 1 KW/cm^2. Two transfer partners were also developed, BiF and BH, which demonstrated both optical gain[2,3] and pulsed lasing[4,5] at 471 and 433 nm, respectively, in lab scale experiments. Neither of these laser systems, however, was able to satisfy the third criterion, and poor power extraction efficiency resulted due to low densities of the active BiF or BH emitters. Under these conditions the NF(a) is destroyed largely by self-annihilation[6] before energy transfer can extract the metastable energy as coherent photons.

Since BiF and BH are both radicals, they are generated *in situ* by dissociation of stable precursors that can be premixed (on-the-fly) with FN_3. In the BiF system, trimethylbismuth (TMB) is used as a volatile source of BiF. While this donor is efficient, its dissociation is slow and byproducts are generated which rapidly quench NF(a). Consequently, before enough BiF can be added to improve power extraction efficiency, the metastable energy store is destroyed by quenching. The pressing need in NF / BiF laser development is therefore to eliminate TMB-induced quenching and enhance the rate of BiF generation.

In the NF / BH system, B_2H_6 has been used to generate BH radicals. In this case, NF($a^1\Delta$) quenching appears to be minimal but the yield of BH radicals per donor molecule is very low.[7] This difficulty stems from the high positive heat of formation of BH, which requires a highly energetic parent molecule. Previously, both diazidoborane and tetraazidodiborane were synthesized

and tested as replacements for diborane,[3] since generation of free BH from these species was thermodynamically accessible due to the high exothermicity of azide-azide annihilation. Diazidoborane, however, turned out to be a low yield donor because the mobile H-atom in this molecule intercepted and terminated the azide reaction by forming linear $HNBN_3$ and N_2. Tetraazidodiborane was a step in the right direction since, in this molecule, the H-atoms are immobilized by bridge bonds. While somewhat higher yields were obtained, this donor was extremely unstable as the electronegative azide groups reduced electron density in the center of the molecule, resulting in destabilization of the critical bridge bonds. Consequently, with respect to NF / BH laser development, the pressing need is to identify a molecule that is similar to tetraazidodiborane with respect to BH generation but with enhanced bridge bond stability. In this way, the critical azide-azide annihilation reaction can complete before H-atoms are released from the immobilizing bridge bonds.

A third approach involves going back a step and attempting to develop an alternative energy transfer system for which donor development is inherently easier to accomplish. In flow tube experiments, Setser[8] observed that addition of I_2 to NF(a) produced NF($b^1\Sigma$), and from this observation concluded that NF(a) must dissociate I_2 as well as pump I-atoms to the $I^*(^2P_{1/2})$ spin-orbit state, similar to the action of $O_2(a^1\Delta)$ in chemical oxygen-iodine lasers.[9] The energy pooling reaction between I* and NF($a^1\Delta$), discovered by Herbelin,[10] would then account for the observed production of NF(b). This explanation also raises the feasibility of an NF / I-atom laser operating at 1315 nm for which donor development would be trivial.

Under the present contract work was done to further the development of advanced BH donors, to improve the yield of BiF from TMB by a precombustion scheme, and to investigate energy transfer kinetics of the NF / I-atom system. The work was done in a pair of previously developed reactor systems where FN_3 was dissociated by a temperature jump, induced either by use of a pulsed CO_2 laser (and SF_6 sensitizer)[1] or by reflection of an incident shock wave[4] generated by a chemical $H_2 + F_2$ explosion. Full details of these reactor systems and the results obtained from them have already been published in the open literature.[1-5,7] This report assumes the reader is already familiar with the methodology used, and a review of the pertinent literature is suggested before attempting to evaluate the results obtained.

NF / BH System

This work involved comparison of two potential BH donors to the baseline system, B_2H_6 or diborane, which previous work[7] established to have a branching ratio of 5 x 10^{-3} in the CO_2 laser triggered reactor. Testing was done by dissociating FN_3 (to generate NF*) in the presence of the donor, while measuring the intensity of BH(A-X) emission at 433 nm.

Pentaborane

A sample of liquid B_5H_9 was provided by Dr. Steve Rodgers of the Air Force Phillips Laboratory at Edwards AFB, CA. A flow of 1 % B_5H_9 in He was obtained by passing He carrier gas through the liquid at ice-water temperature and a regulated pressure of 82 psig. A three-way valve selected either the B_5H_9 / He stream or an equivalent stream of 1 % B_2H_6 in He from a commercial mixed gas cylinder. The selected donor / He gas stream was then directed to either the CO_2 laser-pyrolysis or shock tube reactors by means of an electronic mass flow controller.

In the CO_2 laser driven experiment, the yield of 433 nm emission from B_5H_9 was five times that of equimolar B_2H_6, and identical time profiles were observed. Since the thermodynamics of B_5H_9 is slightly less favorable than B_2H_6 with respect to BH production, this result demonstrates the role of molecular structure in determining the branching ratio. The molecular structure of pentaborane is given as Fig. 1. Heating B_5H_9 to 400°C for 10 ms in route to the reactor eliminated BH production; however, the emission was recovered if HN_3 was added to the flow at the inlet to the capillary oven. These results are similar to prior findings with B_2H_6 and indicate the formation of H-B-N_3 species that are more thermodynamically favorable as donors.

In the shock tube reactor, B_5H_9 did not perform as well as B_2H_6. This difference is thought to reflect the role of higher vibrational temperature in the CO_2 laser triggered reactor, which favors dynamic bond fission over other less useful but thermodynamically more attractive reaction paths. As before, heating B_5H_9 eliminated BH production, but adding HN_3 recovered the signal, if the heating was done on-the-fly. Adding HN_3 and heating upstream of the surge tank, in which the gases were resident for ~ 10^3 seconds before entering the shock tube, was ineffective. Consequently, the active BH donors are shown to be molecules of limited stability.

The improvements achieved using B_5H_9 in place of B_2H_6 were inadequate to define an effective BH donor system.

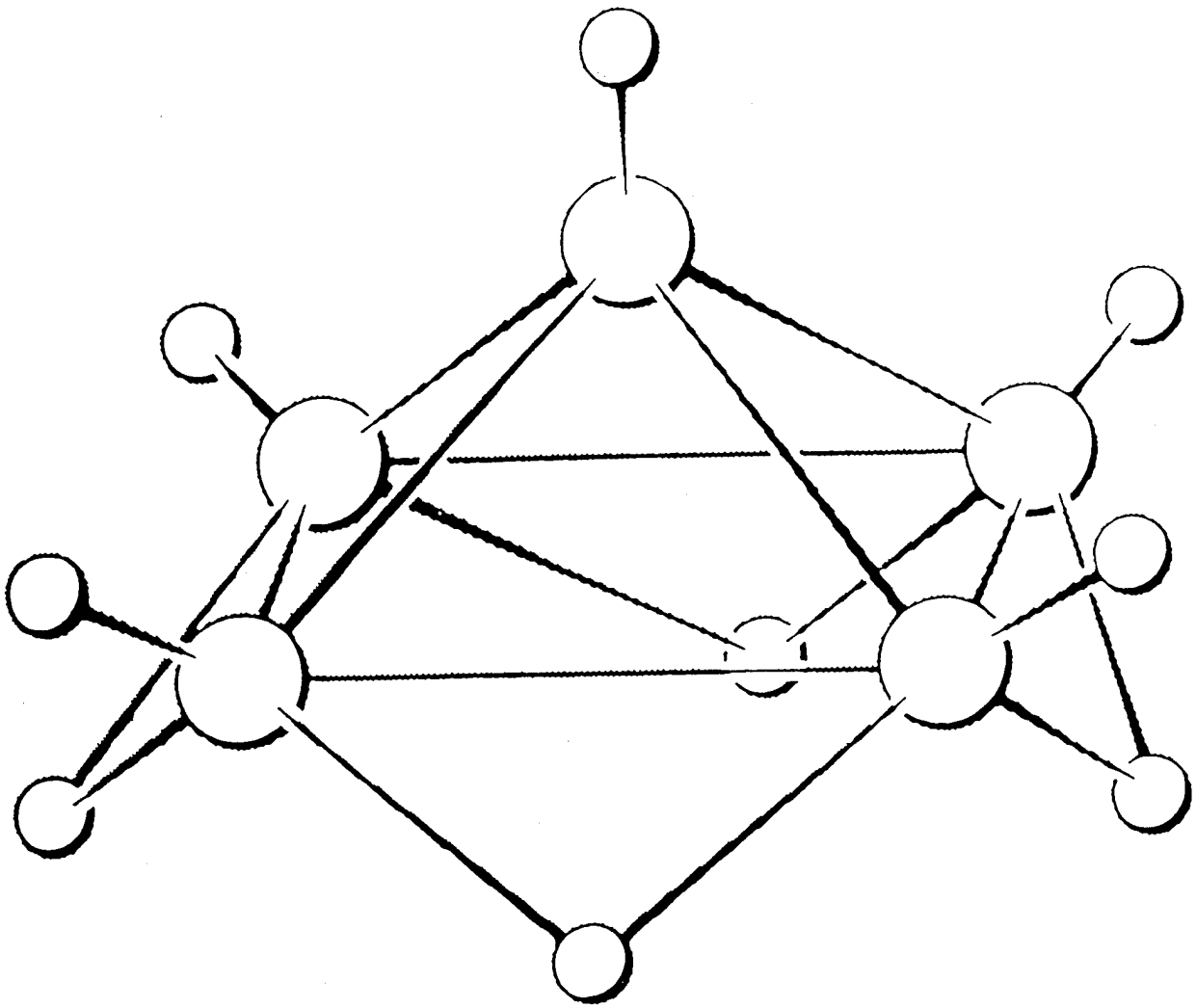

Fig. 1 Molecular structure of pentaborane (B_5H_9).

Dimethyldiazidodiborane

Replacing two of the adjacent azide groups in tetraazidodiborane with more electropositive groups (such as methyl) was thought to be helpful since electron donation would then tend to strengthen the critical bridge bonds. Synthesis of dimethyldiazidodiborane was accomplished on-line by first passing a stream of He through a commercially available sample of $(CH_3)_2$ BBr, then reacting this gas mixture by passage over heated $NaBH_4$ pellets to yield (asymmetrical) dimethyldiborane and

NaBr which condenses out of the flow. An on-line FTIR was used to monitor the reaction and optimal $NaBH_4$ temperature was established as 235°C. The vapor pressure of dimethyldiborane was also measured as 2.5 torr at -65°C. The gas stream carrying dimethyldiborane was subsequently reacted with a mixture of HN_3, Cl_2 and He at 300 K. No direct reactions between HN_3 and Cl_2 or between HN_3 and dimethyldiborane occurred under these conditions. The reaction sequence, with all three reagents present, therefore involved first replacing the terminal H-atoms on dimethyldiborane with Cl-atoms and then exchanging these for N_3 groups to yield HCl byproducts and $(CH_3)_2(BH_2B)(N_3)_2$. Titration of the Cl_2 was critical, since if excess halogen was present the bridge bonds were attacked. The bridge bonds in the product molecule were shown to be considerably more stable than in tetraazidodiborane, as there was no FTIR evidence of decomposition into either $HBCl_2$ or $HB(N_3)_2$. These known byproducts would have occurred if the bridge bonds were not stabilized by the methyl substitutions. Figures 2 (a, b, and c) show the FTIR spectra of dimethyldiborane, and the products of its sequential reactions with Cl_2 and HN_3, respectively. The IR spectra of $(CH_3)_2BBr$ and all the other reagents and byproducts are well known and reported in the open literature.[11,12]

A sample of dimethyldiazidodiborane was trapped at 2.5 torr in the FTIR cell and held at 300 K. The donor decayed with a half life of 15 minutes and left no IR active products; hence the decay mechanism is thought to be polymerization by azide fracture and formation of -B-N = N-B- chains with N_2 byproducts. The decay time, being similar to FN_3, suggests an appropriate level of stability for the laser application since both limited transport and *in situ* dissociation (on the μs time scale) are then feasible.

The synthesis of dimethyldiazidodiborane was optimized but the yield was not quantified, save only that it was less than unity. The starting concentration of $(CH_3)_2BBr$, however, was set at 1 % of the He carrier to match the dilution of B_2H_6 used for baseline comparison purposes. In both the CO_2 laser triggered and the shock initiated reactors, the dimethyldiazidodiborane donor generated 25 to 50 % more BH emission than the diborane reference. Taking into account that only one BH is available from this molecule, compared to two in B_2H_6, and the probable low yield of the synthesis reaction, however, shows that this donor achieved the highest branching ratio of any studied to date. The BH* time profiles from dimethyldiazidodiborane and B_2H_6, however, were different in the shock tube reactor. Here the dissociation time of dimethyldiazidodiborane (~ 4 μs) was a factor of two smaller than for diborane, but an absolute photometry comparison between the two reactors also revealed that efficiency of donor conversion to BH was an order of magnitude larger in the CO_2 laser triggered reactor. These are mixed results with respect to the

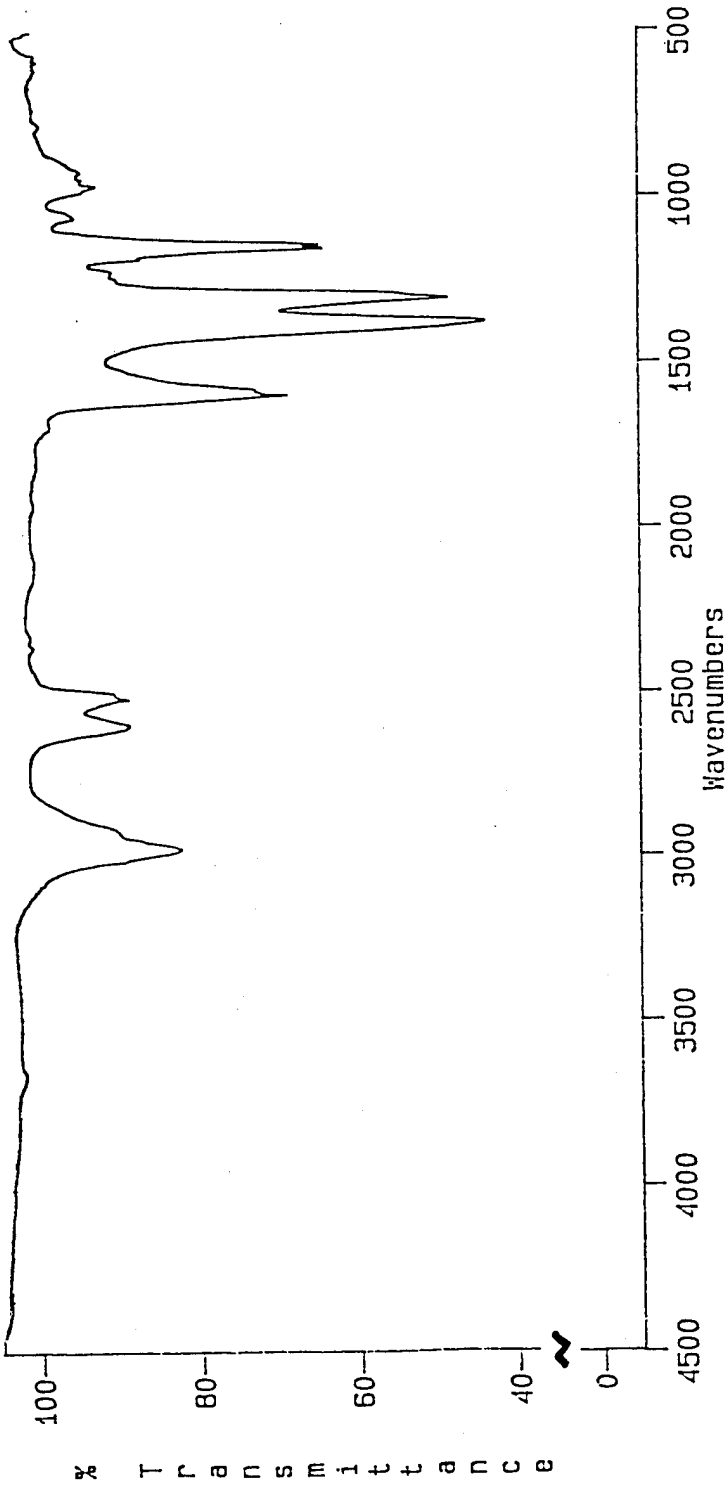

Fig. 2(a) FTIR spectra of $(CH_3)_2(BH_2B)H_2$.

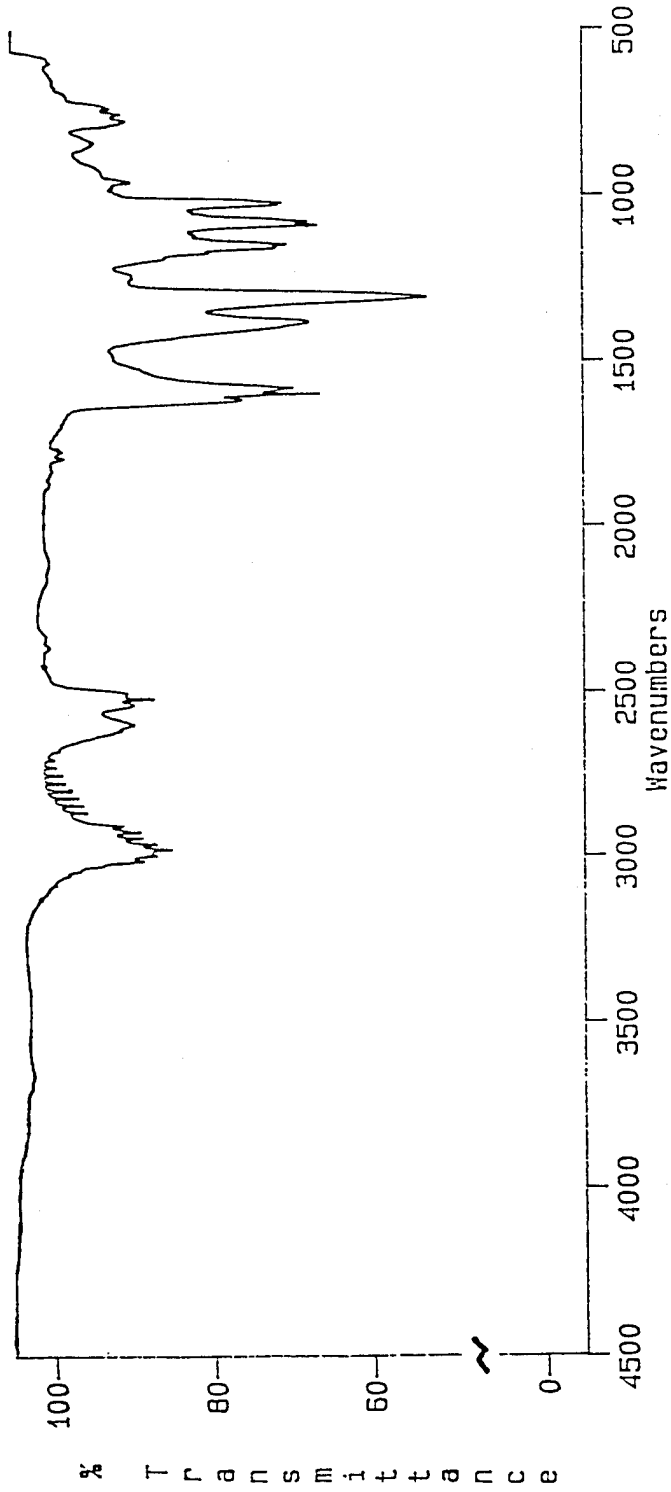

Fig. 2(b) FTIR spectra of $(CH_3)_2(BH_2B)Cl_2$ and HCl byproduct.

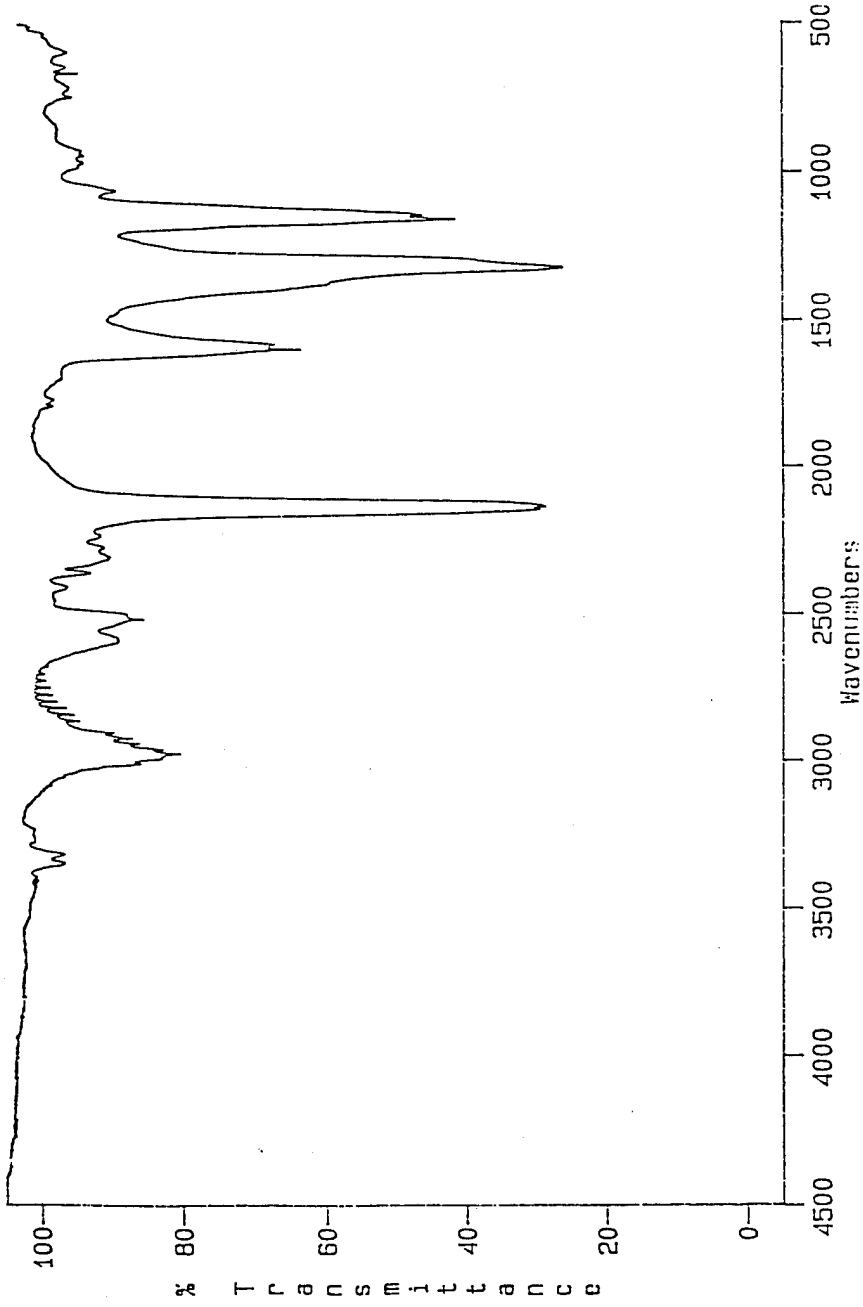

Fig. 2(c) FTIR spectra of $(CH_3)2(BH_2B)N_3)2$ and HCl byproduct.

laser application, and it is clear that additional improvements are required to achieve branching ratios on the order of 10 % or more under shock tube conditions. The shock initiated reactor provides a closer match to a high energy laser device than the CO_2 laser triggered reactor, which relies on a method of initiation that is not scalable.

While methyl substitutions have strengthened the critical bridge bonds and increased the yield of BH, the absolute donor efficiency is still low because the barrier to dissociation of the bridge bonds has not exceeded the (~ 0.5 eV) barrier to azide annihilation.[1] Consequently, while methyl substitutions were a step in the right direction, still more electropositive substituents need to be considered. A potential problem is that such donors will acquire a large dipole moment leading to a host of other difficulties including low vapor pressure, polymerization, and exchange reactions, which occur rapidly between boranes.[13] It is uncertain, for example, to what extent the $(CH_3)_2(BH_2B)(N_3)_2$ rearranged by exchange reactions to the more energetically favorable $CH_3(N_3)(BH_2B)(CH_3)N_3$ configuration, which would not be able to easily generate free BH radicals by annihilation of adjacent azide groups. Use of an electropositive ring structure (in place of the two methyl groups) is therefore thought to be the next step. The necessary *ab initio* investigation required to define the appropriate molecular structure, and the synthetic effort to produce it, however, are beyond the scope of the present contract.

NF / BiF System

The precombustion concept involves mixing TMB donor on the fly with a fuel and oxidizer, and then electrically igniting this mixture in the injection manifold of the shock tube reactor. Reaction between the fuel and oxidizer is intended to generate high temperatures that will dissociate TMB and maintain the resultant Bi-atoms in the vapor phase. The fuel and oxidizer are selected to be stable with TMB, ignite easily, attain high reaction temperature and preferably react away the methyl radicals obtained from TMB dissociation, while at the same time generating byproducts that are not significant quenchers of NF*. Precombustion is not a viable approach for generating BH radicals because the high positive heat of formation of these emitters makes them unlikely products in a thermodynamically controlled reaction.

The prototype precombustion system is $H_2 + F_2$, which experiments quickly demonstrated to be unstable in the presence of TMB, as spontaneous ignitions occurred upon mixing even with O_2 added to quench the H-atom chain carriers. Modeling of this chemical system was, nonetheless, useful in defining critical issues that would occur in other more tractable precombustion concepts. Experiments were also performed to evaluate three more stable systems: $H_2 + NF_3$, $C_2N_2 + O_2$ and $N_2O + CO$, which were each capable of achieving required temperatures, and for which the dominant reaction products (N_2, CO_2, HF) are known[14] to be slow quenchers of NF*.

Precombustion Model

Wilford Smith at SAIC worked with Dr. Ellen Boehmer at Science Center to develop optimized initial conditions and a rate package to model the $H_2 + F_2$ precombustor, using a modified HF chemical laser kinetics code. At 500 K initial gas temperature and 53 torr total pressure, the mole fractions were He (70 %), H_2 (17.6 %), F_2 (8.8 %), TMB (0.15 %) and O_2 (3 %). The rate package included the reaction processes:

$H_2 + F \rightarrow HF + H$	(3E7 / 1.2 / 330)
$H + F_2 \rightarrow HF + F$	(3E6 / 1.5 / 1,680)
$HF + H \rightarrow H_2 + F$	(3E7 / 1.2 / 31,752)
$HF + F \rightarrow H + F_2$	(3E6 / 1.5 / 100,000)
$F_2 + He \rightarrow 2F + He$	(5E10 / 0 / 35,100)

$2F + He \rightarrow F_2 + He$	(5E10 / 0 / 13,354)
$2H + He \rightarrow H_2 + He$	(1E12 / -1 / 0)
$H_2 + He \rightarrow 2H + He$	(1E12 / -1 / 44,710)
$TMB \rightarrow DMB + CH_3$	(1.6E14 / 0 / 44,000)
$DMB \rightarrow MMB + CH_3$	(1.6E14 / 0 / 38,600)
$MMB \rightarrow Bi + CH_3$	(1.6E14/ 0 / 19,000)
$Bi + F + He \rightarrow BiF + He$	(2.1E19 / -5 / 48,500)
$BiF + He \rightarrow Bi + F + He$	(2.9E5 / 0.5 / 65,100)
$Bi + F_2 \rightarrow BiF + F$	(2.2E7 / 0.5 / 0)
$BiF + F \rightarrow Bi + F_2$	(4.2E5 / 0.5 / 25,900)
$Bi + H + He \rightarrow BiH + He$	(8.5E5 / 0.5 / 69,700)
$Bi + H_2 \rightarrow BiH + H$	(1.1E6 / 0.5 / 40,500)
$BiH + H \rightarrow Bi + H_2$	(1.1E6 / 0.5 / 30,000)
$CH_3 + H_2 \rightarrow CH_4 + H$	(6.9E-3 / 2.74 / 9,414)
$H + CH_4 \rightarrow H_2 + CH_3$	(0.013 / 3 / 8,033)

The temperature dependent rate coefficients (A / B / C) for each reaction are given in the Arrhenius form ($k = A\ T^B\ e^{-T/C}$) in units of liter / mole-s and the calculation was initiated by assuming ~ 0.1 % of the F_2 was dissociated at t = 0. Figures 3(a-g) display the calculated temperature, pressure and species concentrations vs logarithmic time out to 1 ms. These results show that TMB is rapidly converted to Bi-atoms and BiF at 3500 K, but the CH_3 radicals are not recombined to CH_4. Consequently, there is an issue in regard to potential quenching of NF* by CH_3 byproducts. A more detailed rate package and the associated references relative to this precombustion concept are reproduced in the Appendix of this report.

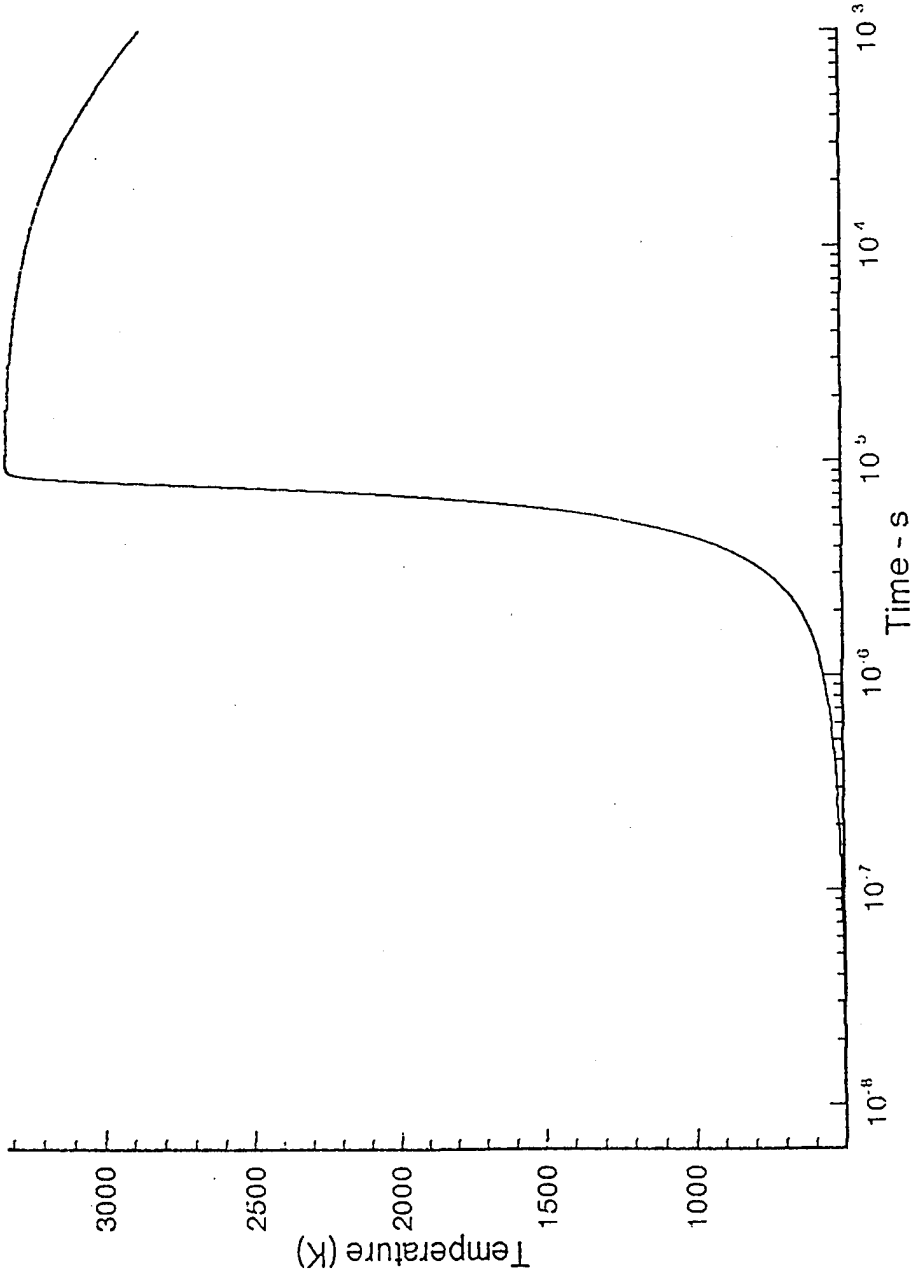

Fig. 3(a) Precombustion modeling, temperature time profile.

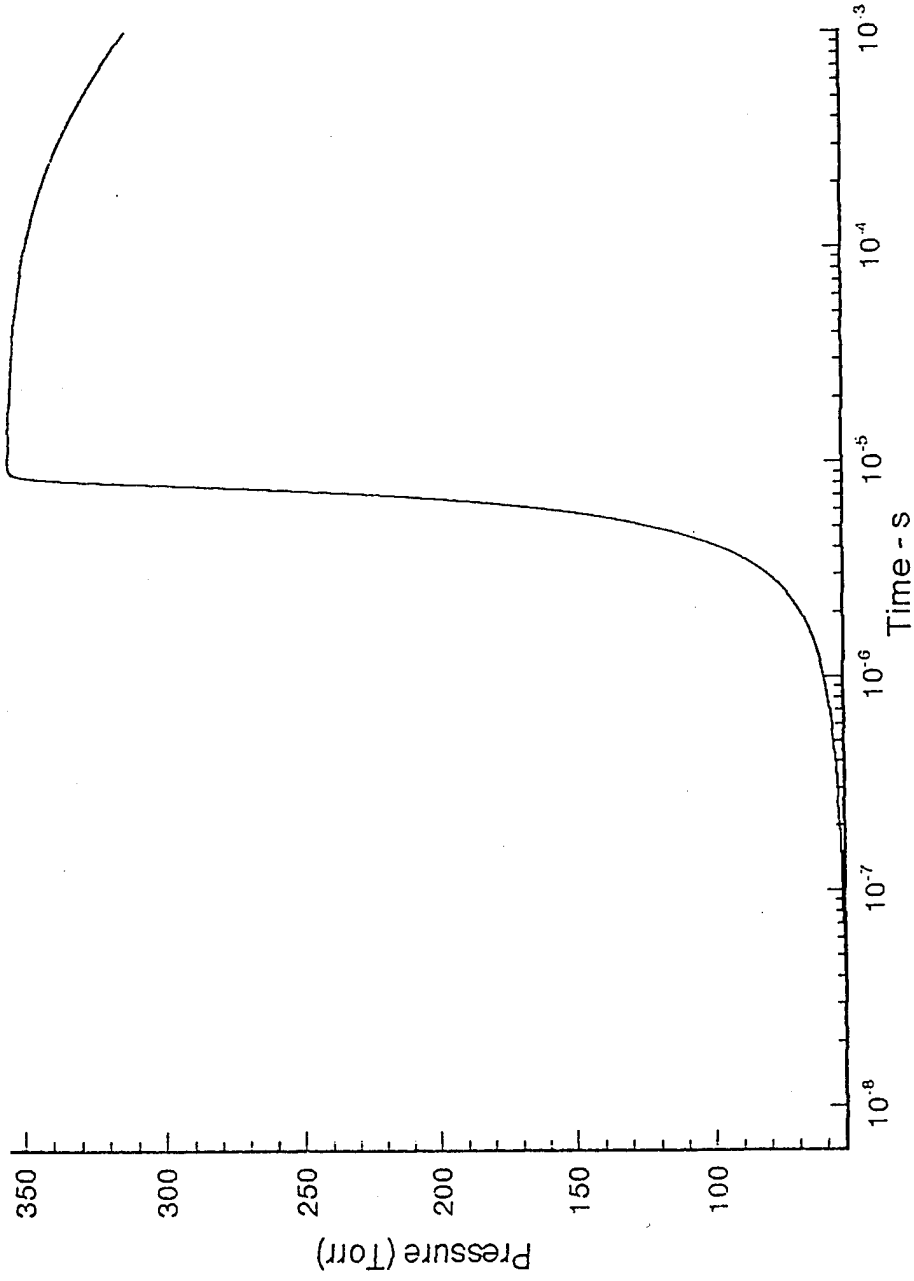

Fig. 3(b) Precombustion modeling, pressure time profile.

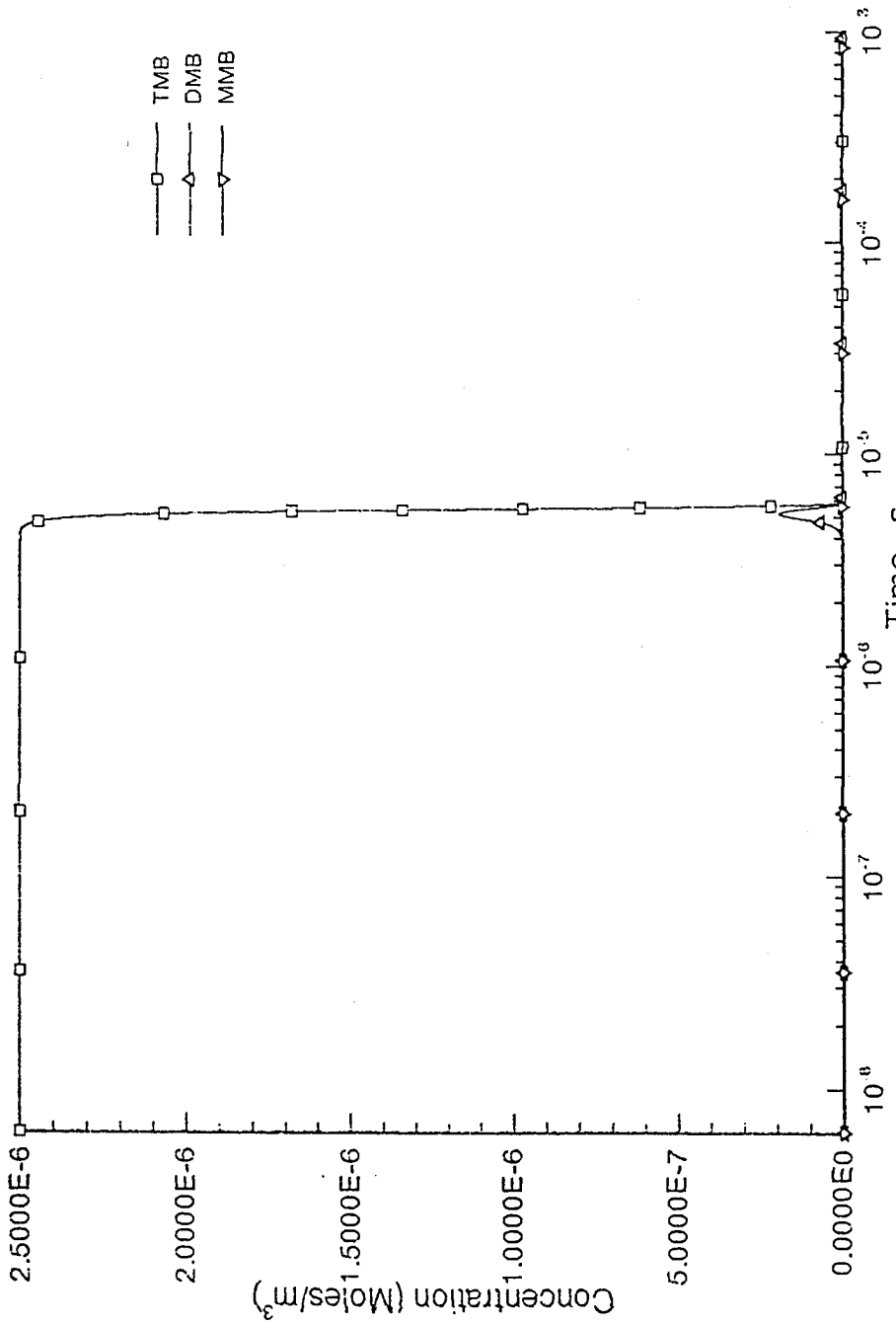

Fig. 3(c) Precombustion modeling, time profiles of methyl-bismuth species.

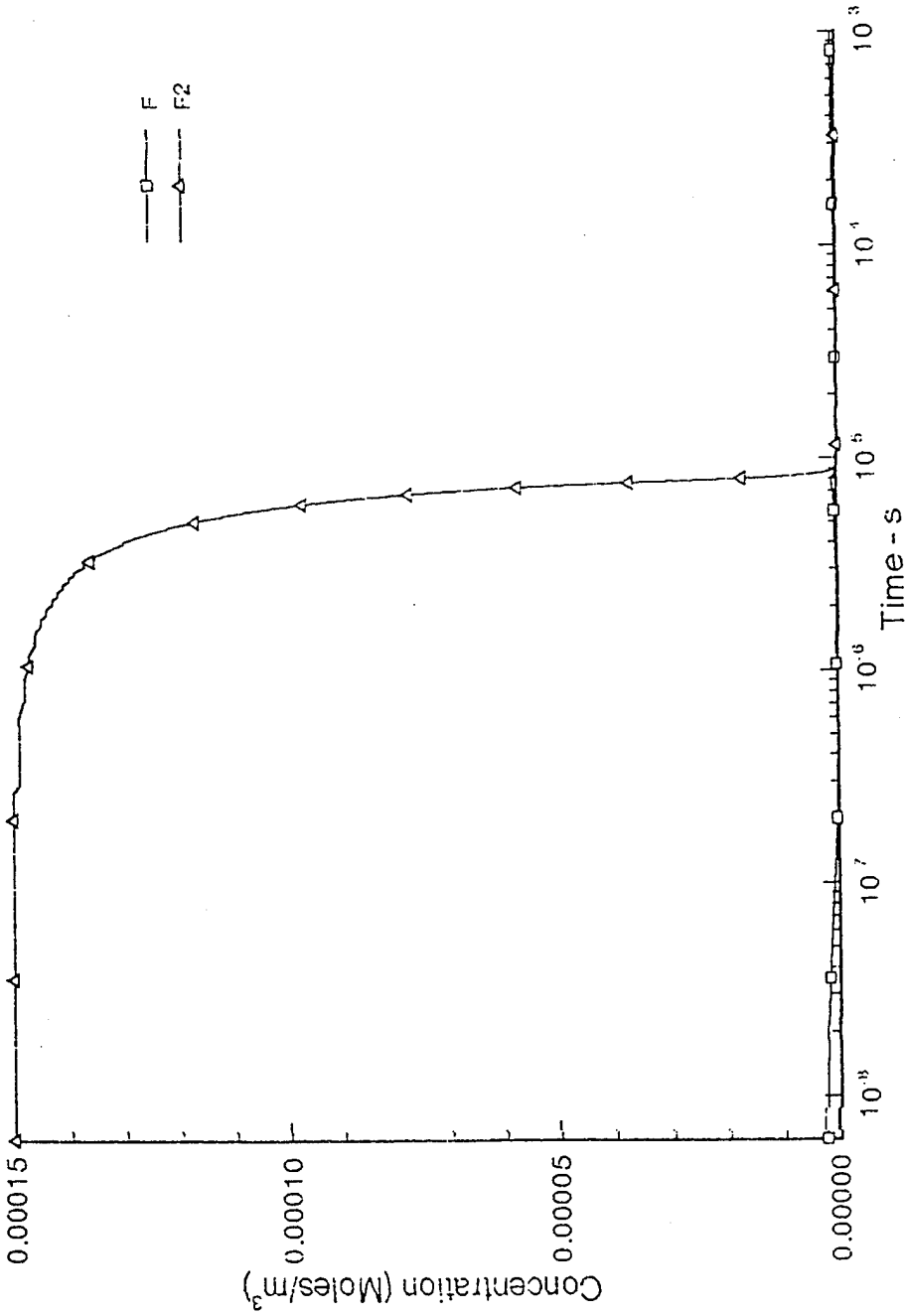

Fig. 3(d) Precombustion modeling, time profiles of F-atoms and F_2.

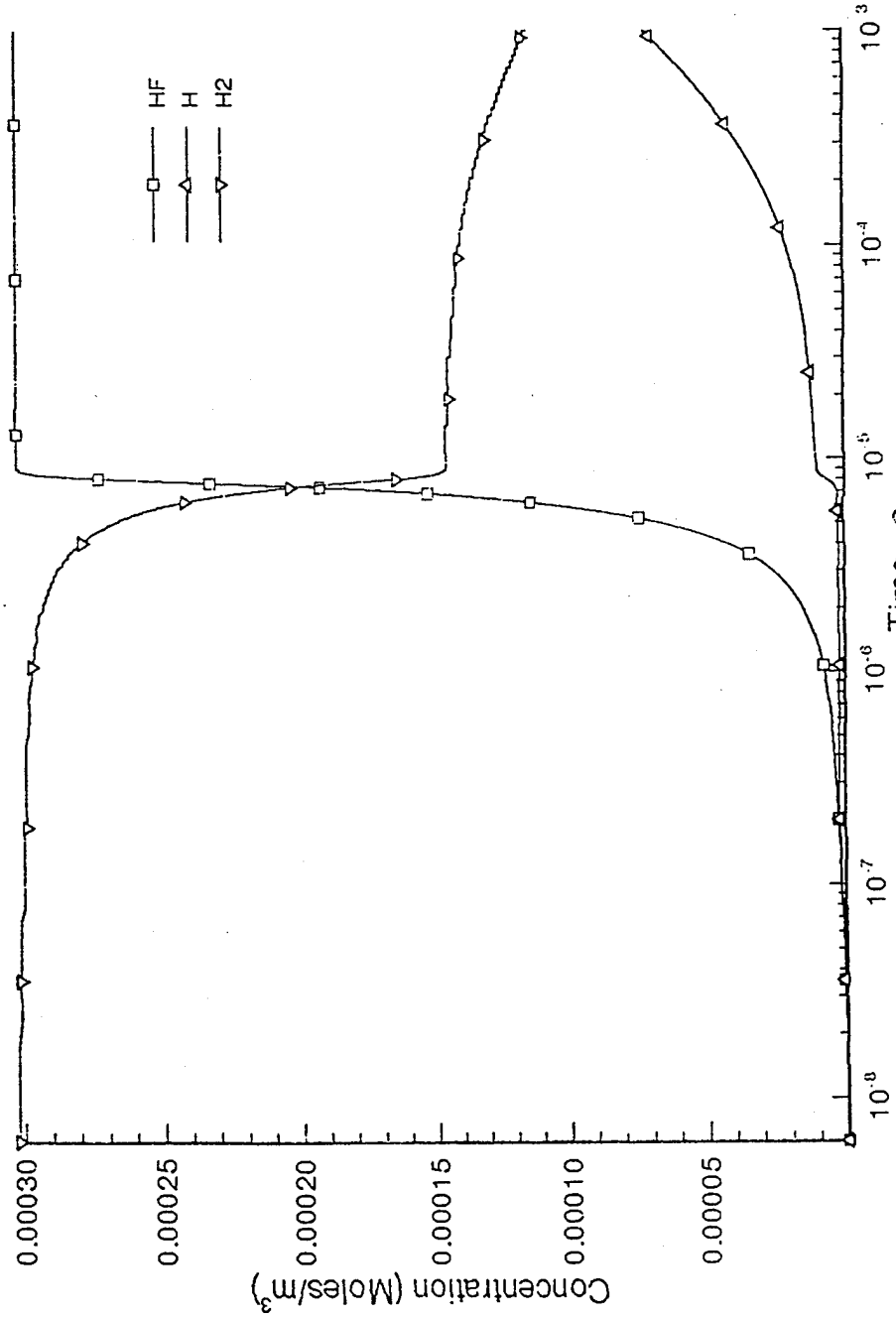

Fig. 3(e) Precombustion modeling, time profiles of H-atoms, H_2 and HF.

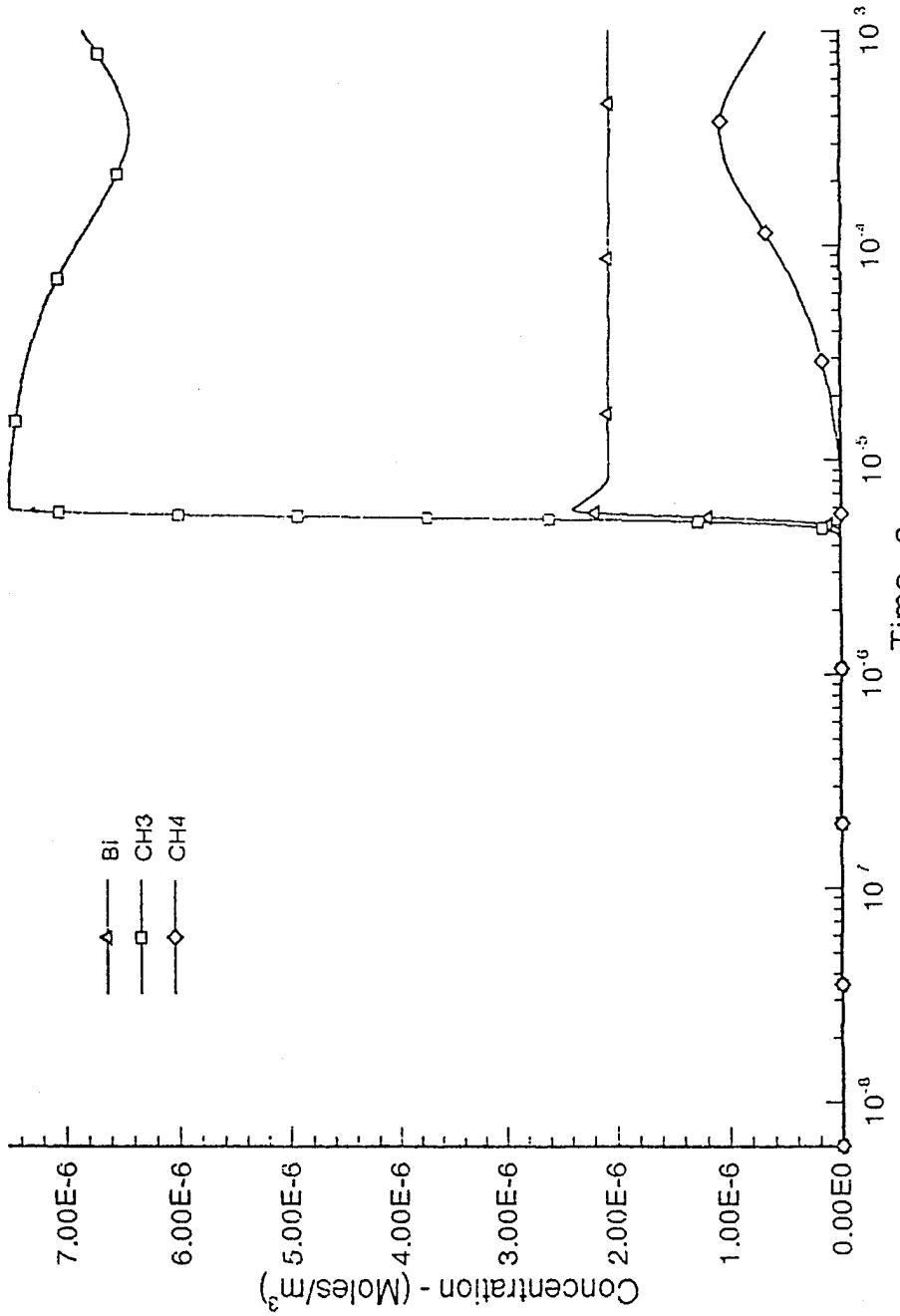

Fig. 3(f) Precombustion modeling, time profiles of Bi-atom, CH_3 radical and CH_4.

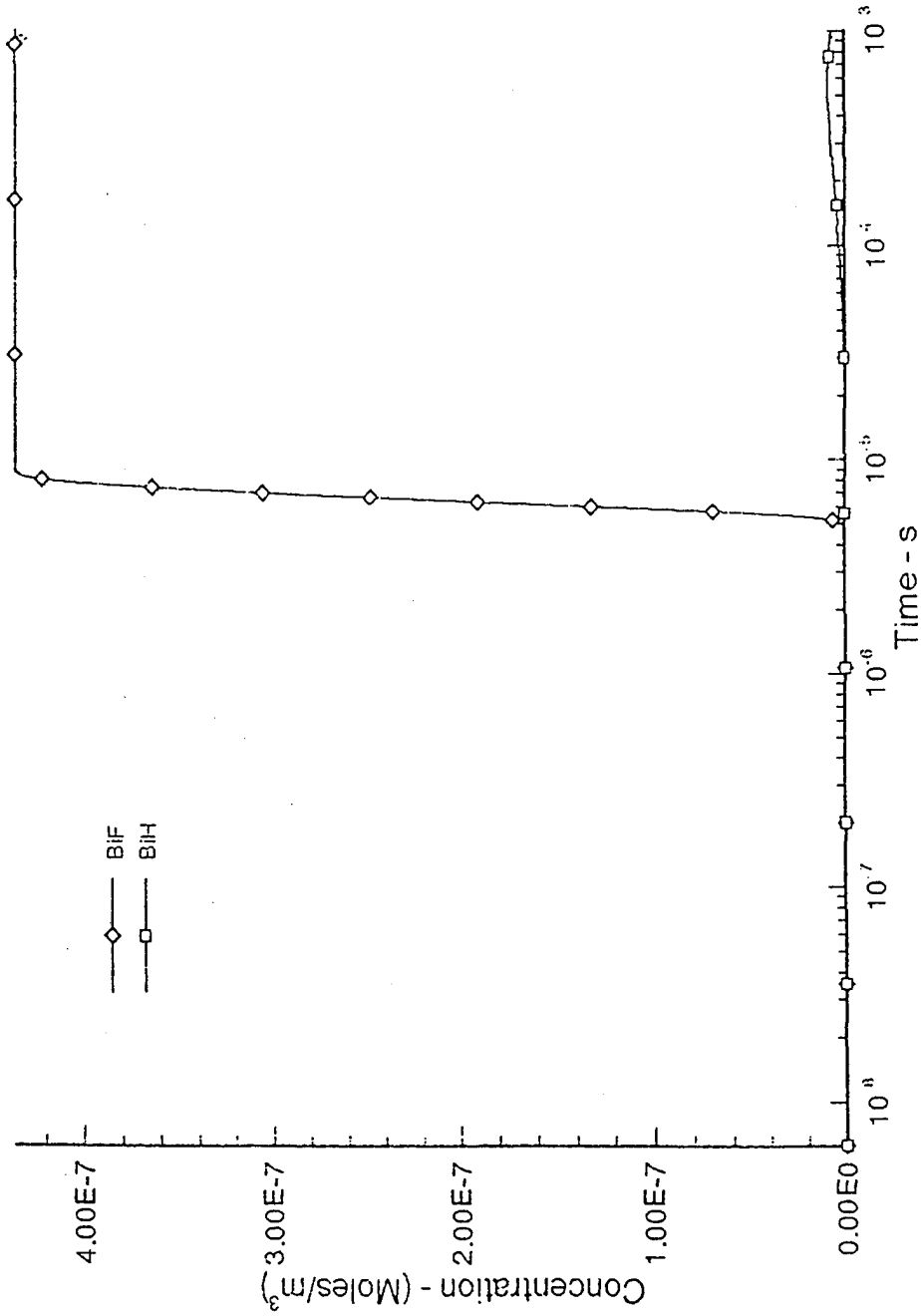

Fig. 3(g) Precombustion modeling, time profiles of BiF and BiH.

Quenching of NF by CH_3*

Experiments were performed in the CO_2 laser triggered reactor at high laser fluence and low pressure to optimize the yield of F-atoms from multiphoton dissociation of SF_6. Fixed FN_3 and variable CH_4 flows were added to the SF_6 and He gas in the reactor to generate NF* and CH_3 radicals by the fast $F + CH_4 \rightarrow CH_3 + HF$ reaction. In this experiment, the decay of NF* is dominated by self-annihilation and quenching by reaction with CH_3 radicals. The known rates of NF* quenching by CH_4 and HF are negligible by comparison. Also, CN* emission (which tracks the NF* concentration) was optically measured rather than NF*, because of the presence of interfering emissions at the 874 nm wavelength. Figure 4(a) shows the titration curve, which establishes a F-atom yield of 4.4×10^{15} / cm^3. Figure 4(b) shows a Stern-Volmer plot of the decay rate vs inferred CH_4 concentration. For low values of CH_4 addition, CH_3 was taken as equal to the measured CH_4 concentration since F-atoms were in excess (dots), whereas for higher CH_4 additions (crosses) the CH_3 concentration was taken as proportional to the CN* emission using a calibration factor developed at lower CH_3 concentrations. The linear relationship between the decay rate and CH_3 concentration yields a rate constant of $\sim 9.2 \times 10^{-12}$ cm^3/s, with an estimated error of $\pm$ 20 %, due to scatter in the data.

The magnitude of NF* quenching by CH_3 is comparable to NF* quenching by undissociated TMB measured by Setser,[14] and is much less than the inferred rate of NF* quenching in the laser system where DMB and MMB are also present.[4] The difficulty with use of raw TMB as a donor is therefore associated with the intermediate dissociation products. The modeling calculations performed above, however, indicate that these will be effectively removed if the reaction temperature is high enough. Quenching of NF* by CH_3 radicals will occur, but since initial TMB will be at least an order of magnitude smaller than NF*, the net rate of metastable deactivation will be no worse than self-annihilation. The success of a precombustor scheme therefore depends on other factors which can best be addressed through experimental investigation.

Precombustion Reactor

The shock tube reactor admits the donor and FN_3 gas flows into the shock channel through two oppositing (independent) manifolds. To accomplish precombustion, the donor channel was modified by the installation of a row of spark plugs and a separate pulsed high voltage power supply. The solenoids controlling the flows of the precombustion mix were also wired separately from the solenoids that control the FN_3 flow so that separate valve timing could be established.

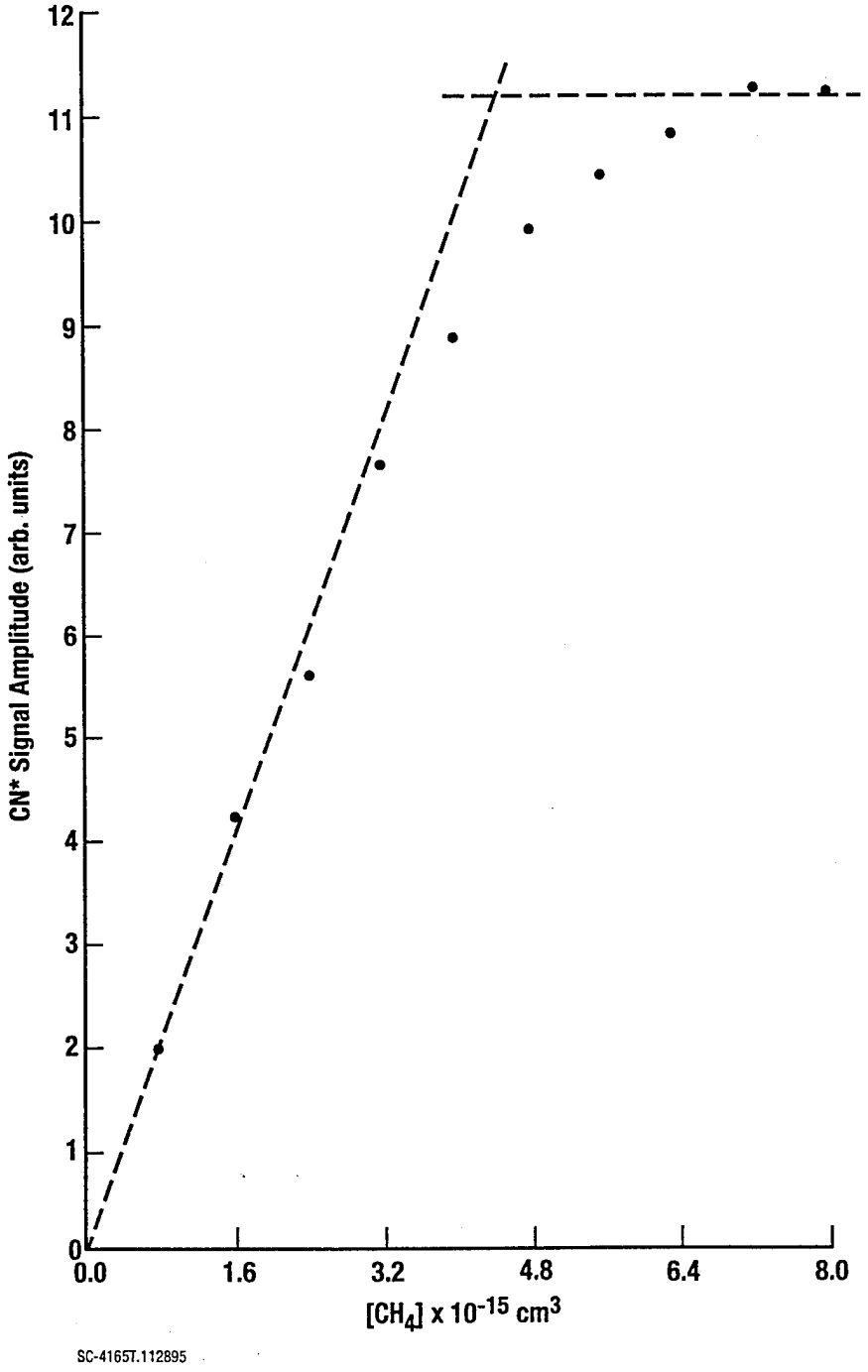

Fig. 4(a) Titration curve, $F + CH_4 \rightarrow HF + CH_3$.

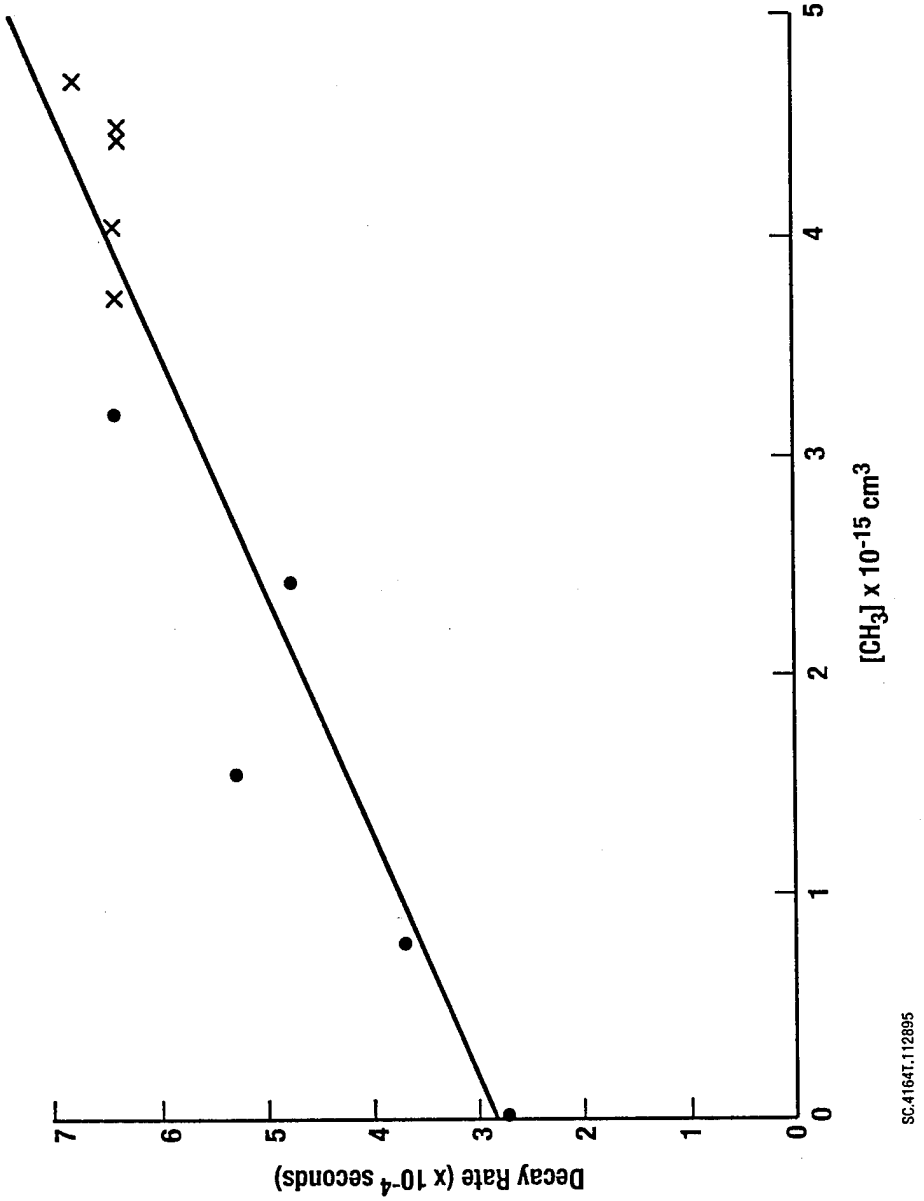

Fig. 4(b) Stern-Volmer analysis of NF* quenching by CH_3 radicals.

The sequence of events in a typical shot involved first opening the valves to admit precombustion gases to the manifold and then opening the FN_3 valve after a time delay equivalent to half a valve cycle. Both sets of valves stayed open for equal durations; hence the precombustion valve closed before the FN_3 valve. Because of this syncopation, FN_3 is excluded from the precombustion manifold, which bleeds down to the pressure of the shock channel, and the shock channel is filled with only FN_3 by the time the last valve closes. At this point, the high voltage to the precombustor is fired and the separate high voltage used to trigger the shock tube driver is triggered (later) after a variable time delay. The purpose of this last delay was to synchronize arrival of the incident shock with gases that are injected from the precombustion manifold into the shock channel due to a pressure jump driven by heat release of the precombustion reaction. To prevent back flow from the precombustor, an electronically activated check valve was employed that sealed off the manifold from its gas supplies half a valve cycle before ignition.

A fast PZT detector was employed to monitor the pressure in the precombustion manifold, and for typical reaction conditions (designed to achieve temperatures of 3500 K) the pressure rose from an initial 50 torr to about 600 torr in less than 0.2-0.5 ms (reaction time) before decaying exponentially with a 2-3 ms time constant that was characteristic of the manifold bleed down through injection orifices. The shock was typically synchronized to arrive at the point where decaying manifold pressure was between one-third and two-thirds of its peak value. The operation of the shock tube reactor was in all other respects equivalent to the previous NF / BiF laser experiments.[5] Appropriate mixing in the shock channel was evidenced by visual observations of the spatial extent of 450 nm chemiluminescence through an interference filter. The principal time resolved optical diagnostic used to evaluate the precombustion schemes was a PMT filtered to respond to BiF(A-X) emission that was coupled to a fast preamplifier and storage oscilloscope with a delayed time base synchronized to the shock tube driver. A gated optical multichannel analyzer (OMA) was also employed to spectroscopically identify the emitting molecules.

H_2 + NF_3 Precombustor

In this reaction system, it is necessary to operate with H_2 in excess, since otherwise the Bi-atoms liberated by decomposition of TMB will be oxidized to higher fluorides than BiF, which are not useful for lasing purposes. The TMB was carried in the H_2 stream and there was no evidence of prereaction upon mixing the NF_3 and H_2 / TMB streams at the precombustor inlet. Electrical ignition of the H_2 / NF_3 / TMB mixtures was facile and some chemiluminescence was observed in the shock channel as the reaction products were injected. Only BiF(A-X) emission was detected in

the OMA scan and the strength of this emission increased proportional to TMB concentration as well as in response to FN_3 addition and arrival of the incident shock. From the time profiles of the chemiluminescence under various conditions of operation, however, it became clear that the precombustion products (including both H and Bi-atoms) react spontaneously with FN_3 upon mixing. Consequently, this reaction scheme is ill-suited for a laser demonstration, because the yield of NF* from a slow mixing initiated dissociation of the azide is reduced dramatically by self-annihilation. Attention was therefore focused on other precombustion systems which allowed more stable mixing of the products with FN_3, and subsequent shock dissociation to yield higher NF* concentrations. Attempts to inject behind the shock were ineffective because the pressure increase due to shock reflection in the test channel was greater than the pressure increase due to precombustion in the donor manifold.

C_2N_2 + O_2 Precombustor

In this system, TMB was carried in a separate He stream and then merged on-the-fly with the precombustion reagents at a 3-way mixer. No problems with prereaction occurred, but electrical ignition was difficult unless 5-10 % of H_2 was added to the gas stream. Use of increased spark energy decreased but did not eliminate the requirement for H_2 addition. Best results were obtained under stoichiometric conditions, and once ignited, the precombustor fuels burned rapidly (similar to the NF_3 system above) but there was no chemiluminescence detected upon donor injection or mixing with FN_3 in the shock channel. Upon shock excitation, however, intense Bi-atom emission at 472 nm was detected while the BiF(A-X) bands were strongly suppressed. It is likely that this result occurs because the precombustor generates Bi carriers of the form OBiCN, as the most thermodynamically favored product. This species is stable in the presence of FN_3 but is likely to react with NF* (following shock excitation) according to the reactions

$$NF + OBiCN \rightarrow ONF + BiCN$$

$$NF + BiCN \rightarrow NF(CN) + Bi$$

The Bi-atoms so produced are not converted to BiF because F-atoms are more strongly bound to N-atoms than to Bi-atoms. Hence, the F-atom exchange reaction

$$NF + BiF \rightarrow NF_2 + Bi$$

is more favorable than the opposing reaction

$$NF + Bi \rightarrow N + BiF.$$

Consequently, if BiF is not generated by some form of auxiliary chemistry it will not be formed as a result of Bi-atoms reacting with NF*. This finding has significant implications with respect to use of vaporized bismuth metal as a BiF precursor.

N_2O + CO Precombustor

In this system, TMB was carried by the CO gas stream and best results were obtained under slightly oxidant rich conditions. No difficulties were encountered with prereaction, but approximately 20 % H_2 addition was required to achieve facile electrical ignition, independent of spark energy. This combustion system is known to proceed slowly in the absence of a catalyst.[15] There was no chemiluminescence associated with donor injection or reaction with FN_3, and upon shock excitation an order of magnitude improvement of the BiF yield was noted.

The most thermodyamically favored product in this precombustion system is BiO, which is likely to have a dark reaction with the azide

$$BiO + FN_3 \rightarrow FBiO + N_3$$

to yield a product that is stable until NF* appears following shock excitation. Then BiF is recovered according to the exothermic reaction

$$NF + FBiO \rightarrow ONF + BiF$$

and the BiF emitter is subsequently excited by energy transfer and pooling from the NF* metastables. As shown in Fig. 5, the emission spectrum resulting from shock heating of FN_3 and the N_2O / CO / H_2 / TMB precombustion products contains both BiF(A-X) and Bi-atom emissions, as well as an underlying continuum that was not present in the chemiluminescence spectrum obtained without precombustion.[4] This emission occurs at a wavelength that is appropriate for species containing CN radicals.[16]

Lasing experiments were performed under (precombustion) conditions which duplicated the prior NF / BiF laser demonstration and no BiF emission was observed to escape the laser cavity. This result is symptomatic of intracavity absorption, most likely associated with the carrier of the

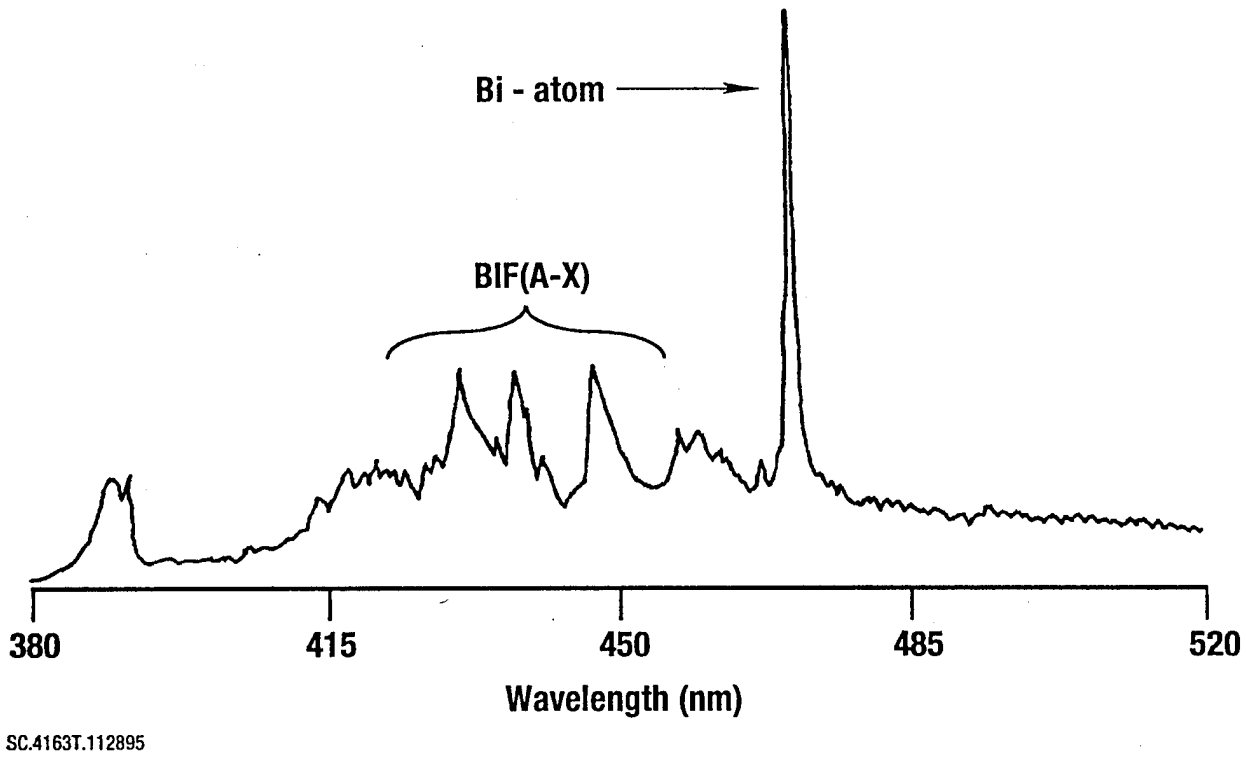

Fig. 5 Effect of precombustion on BiF(A-X) chemiluminescence spectra.

continuum emission. Therefore, it appears that although N_2O + CO precombustion enhances the yield of BiF, it also generates an optically absorptive byproduct which negates any chance of lasing in this gas medium.

Because the reaction concepts tested above cover a range of C-N-O-H chemistries, it does not seem likely that an alternative reaction system will be identified that is suitable. Since either C or N carrying species must be eliminated to prevent formation of absorptive byproducts, the choice is between C-O-H systems which are not hot enough, or N-O-H systems which derive their heat release from H_2O formation by trimolecular reactions that are slow at reduced pressure. Consequently, the concept of using a chemical precombustor to improve the yield of BiF from TMB appears to have reached its limit. These results, however, do not rule out potentially viable donor concepts based on either a thermal process driven by heat exchange (in an inert gas diluent) or the *ab initio* design and synthesis of alternative BiF donors, such as $(CF_3)BiF_2$ which may thermally crack to CF_4 and BiF.

NF / I-Atom System

Work on this concept has been fully detailed in a publication entitled "Energy Transfer from High Densities of Metastable NF to Iodine" that has been submitted to the Journal of Physical Chemistry for publication in the open literature. The experiments were performed in the shock tube reactor, using He to carry I_2 from a saturation cell in place of TMB, and optical diagnostics were employed to measure the time profiles of NF(a,b), I* and I_2 following shock excitation of FN_3 / I_2 / HF / He gas mixtures. The results were anchored to a gasdynamic and chemical kinetics model of the reaction process based on the mechanism shown below.

$\Delta + FN_3 \rightarrow NF(a) + N_2$	198,200 / s	(1a)
$\Delta + FN_3 \rightarrow NF(b) + N_2$	1,800 / s	(1b)
$NF^* + I_2 \rightarrow NF(X) + I_2$	2.2×10^{-10} cm^3 / s	(2a)
$NF^* + I_2 \rightarrow NF(X) + 2\ I$	4.4×10^{-11} cm^3 / s	(2b)
$NF^* + M \rightarrow 2\ M$	3.0×10^{-12} cm^3 / s	(3)
$NF(a) + I \rightarrow NF(X) + I^*$	8.5×10^{-11} cm^3 / s	(4a)
$NF(a) + I \rightarrow NF(X) + I$	4.3×10^{-12} cm^3 / s	(4b)
$NF(a) + I^* \rightarrow NF(b) + I$	6.0×10^{-11} cm^3 / s	(5a)
$NF(b) + I \rightarrow NF(a) + I^*$	6.0×10^{-11} cm^3 / s	(5b)
$NF(b) + HF \rightarrow NF(a) + HF$	1.4×10^{-12} cm^3 / s	(6)
$I^* + HF \rightarrow I + HF$	7.2×10^{-12} cm^3 / s	(7a)
$I^* + I_2 \rightarrow I + I_2$	3.0×10^{-11} cm^3 / s	(7b)
$I^* + M \rightarrow I + M$	7.5×10^{-11} cm^3 / s	(7c)

In this rate package, M equals the combined concentration of all the NF species present including FN_3, NF(X,a,b) and the products of self-annihilation. Consequently, M is treated as a constant equal to the initial azide concentration. Figure 6 shows the time profiles of NF(a,b), I* and ground state I-atoms that were obtained by calculation after the rate package was anchored to data. Although the NF* rapidly dissociates I_2, and energy transfer to I-atoms is both fast and efficient, lasing was not achieved in this system because the I* concentration never exceeded half of the

ground state I-atoms. The primary cause of this difficulty is attributed to fast E-V quenching of I* by the NF-related species taken as a group. Since this limitation is inherent to the concept, there appears to be little chance of developing a laser based on the NF / I-atom transfer concept.

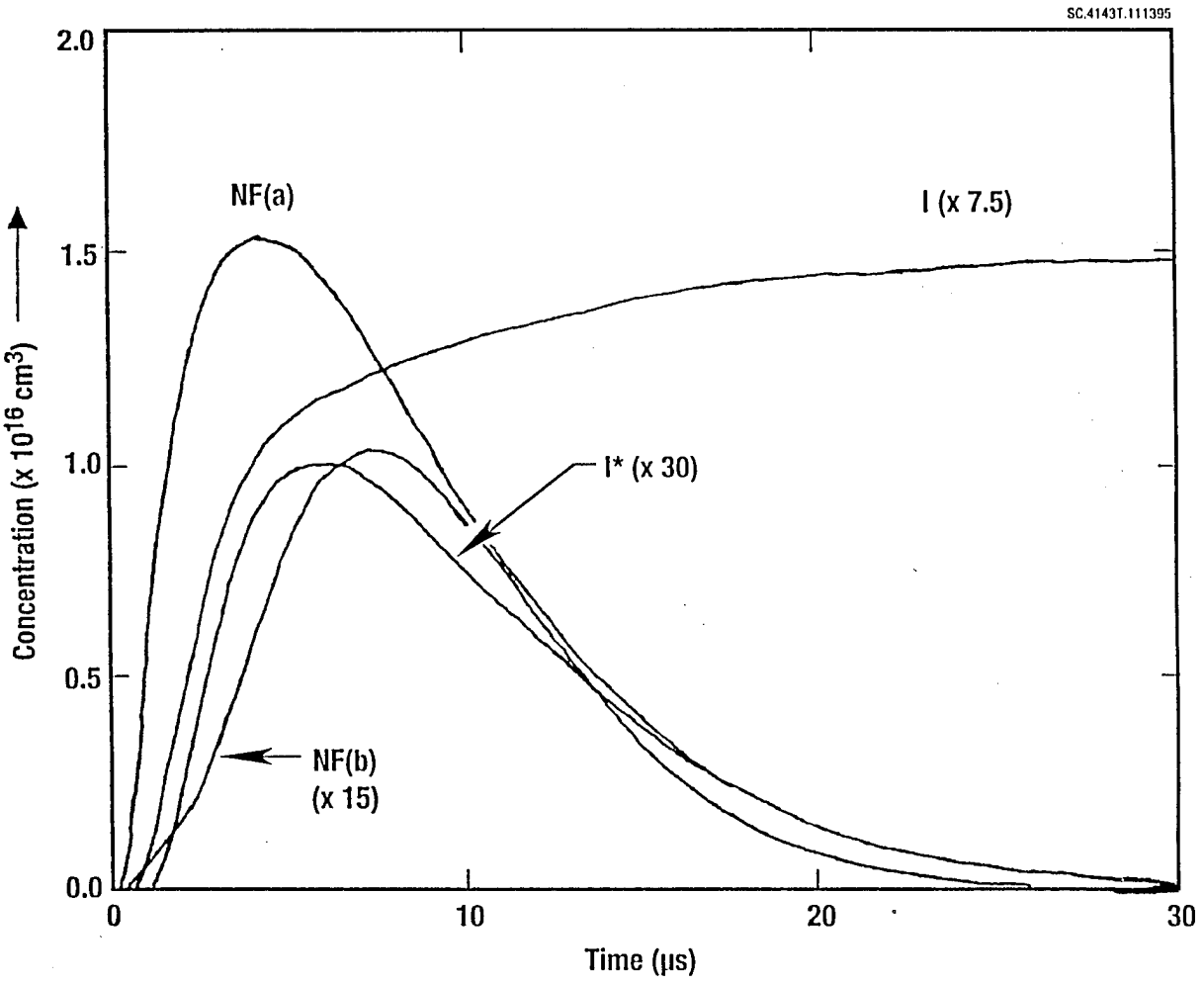

Fig. 6 Kinetic time profiles of key species in the NF / I-atom system.

Recommendation

The effort to develop a visible wavelength chemical laser spans more than two decades and encompasses the work of several investigators. While the government's program, from the beginning, focused on parallel development of scalable metastable generators and suitable energy transfer systems, the need to develop a scalable donor technology has not been realized until very recently, and this is the first contract to address that critical issue. Ability to generate Torr-level concentrations of NF* was not achieved until 1989, after roughly fifteen years of effort. In the following five years, two effective transfer systems were developed to the point of lab scale gain and lasing demonstrations enabled by access to these high metastable concentrations as well as the preceding work (by others) on transfer systems that couple to NF*. The effort to develop a scalable donor technology is no less challenging because of the constraints placed upon it by solutions (now in hand) that address the prior issues of metastable generation and inversion by energy transfer.

Under the present contract we have laid a basis for developing an effective BH donor, the inherent difficulties with the BiF precombustion concept were exposed, and we have shown that coupling NF* to I-atoms is not a viable approach to a new chemical laser. These results leave open the possibility of an effective BiF donor based on the same three step (sequential) approach that is needed to develop a fully satisfactory BH donor. First, a significant program of *ab initio* calculations is required to identify a donor molecule of suitable stability, which preferentially fragments into the desired emitters and benign by-products. Second, a chemical synthesis program will be needed to prepare limited quantities of the optimized donor, since in all probability, if the magic bullet were either commercially available or easily synthesized it would already have been identified. Third and finally, the synthesized donor needs to be tested at high NF* density by methods used in our laboratory. To insure success, some level of involvement with the synthesis and testing teams will be required during the *ab initio* phase to guide the investigation towards parent molecules that can be physically realized, and which are suitable for the laser application.

Such a program will be neither fast nor inexpensive, and the government will have to conduct a serious evaluation to determine if the requirement for a visible chemical laser is a high enough priority to justify the required investment. The cost and schedule of this three-step approach is, nonetheless, still small compared to the cost and schedule of completing development of a visible wavelength high-energy laser system, once a fully satisfactory chemical gain medium has been identified and demonstrated. It does not appear at all likely, however, that a quick breakthrough can reasonably be expected from the current state of development by means of a single effort or the efforts of several investigators working in parallel.

References

1. D.J. Benard, B.K. Winker, T.A. Seder and R.H. Cohn, *J. Phys. Chem.* **93** (1989) 4790.

2. D.J. Benard and B.K. Winker, *J. Appl. Phys.* **69** (1991) 2805.

3. D.J. Benard, E. Boehmer, H.H. Michels and J.A. Montgomery, *J. Phys. Chem.* **98** (1994) 8952.

4. D.J. Benard, *J. Appl. Phys.* **74** (1993) 2900.

5. D.J. Benard and E. Boehmer, *Appl. Phys. Lett.* **65** (1994) 1340.

6. E. Quinones, J. Habdas and D.W. Setser, *J. Phys. Chem.* **91** (1987) 5155.

7. E. Boehmer and D.J. Benard, *J. Phys. Chem.* **99** (1995) 1969.

8. K.Y. Du and D.W. Setser, *J. Phys. Chem.* **94** (1990) 2425.

9. D.J. Benard, W.E. McDermott, N.R. Pchelkin and R.R. Bousek, *Appl. Phys. Lett.* **34** (1979) 40, and references.

10. J.M. Herbelin, M.A. Kwok and D.J. Spencer, *J. Appl. Phys.* **49** (1978) 3750.

11. S.D. Ross, Inorganic and Raman Spectra (McGraw Hill, 1972).

12. C.J. Pouchert, Aldrich Library of FTIR Spectra, Vol. 3 (1989).

13. H. Takeo, M. Sugie and C. Matsumura, *J. Molec. Spectrosc.* **158** (1993) 201.

14. J. Habdas and D.W. Setser, *J. Phys. Chem.* **93** (1989) 229.

15. C.P. Fennimore and R. Kelso, *J. Am. Chem. Soc.* **72** (1950) 5045.

16. B. Rosen, Selected Constants and Spectroscopic Data Relative to Diatomic Molecules (Pergammon, 1970).

APPENDIX

DONOR PRECOMBUSTION CHEMISTRY

E. Boehmer

Rockwell International Corp., Science Center
1049 Camino Dos Rios
Thousand Oaks, CA 91360

Abstract

Previous shock tube investigations have shown that TMB dissociation is slow even at elevated temperatures. In addition, the dissociation byproducts are efficient NF^* quenchers. This study presents conditions for a H_2/F_2/TMB precombustor, which allows for larger TMB dissociation yields and for the conversion of reactive quenchers into benign byproducts (CH_4 and HF). Also, under hydrogen rich conditions Bi is likely to be converted to BiH_3, which is a volatile Bi atom source.

Introduction

Shock tube studies on $Bi(CH_3)_3$ (TMB) as Bi source in thermochemical laser systems containing $NF(a^1\Delta)$ as energy carrier have revealed the following facts: (i) The yield of Bi atoms after thermally initiated dissociation of TMB is surprisingly low, and (ii) in addition, TMB yields byproducts that are very efficient quenchers.[1] For each Bi atom three CH_3 radicals are produced. Consequently, the main goal of this study is to investigate pre-combustor conditions, which allow for larger TMB dissociation yields and the conversion of CH_3 and other radicals such as H and F atoms into benign quenchers.

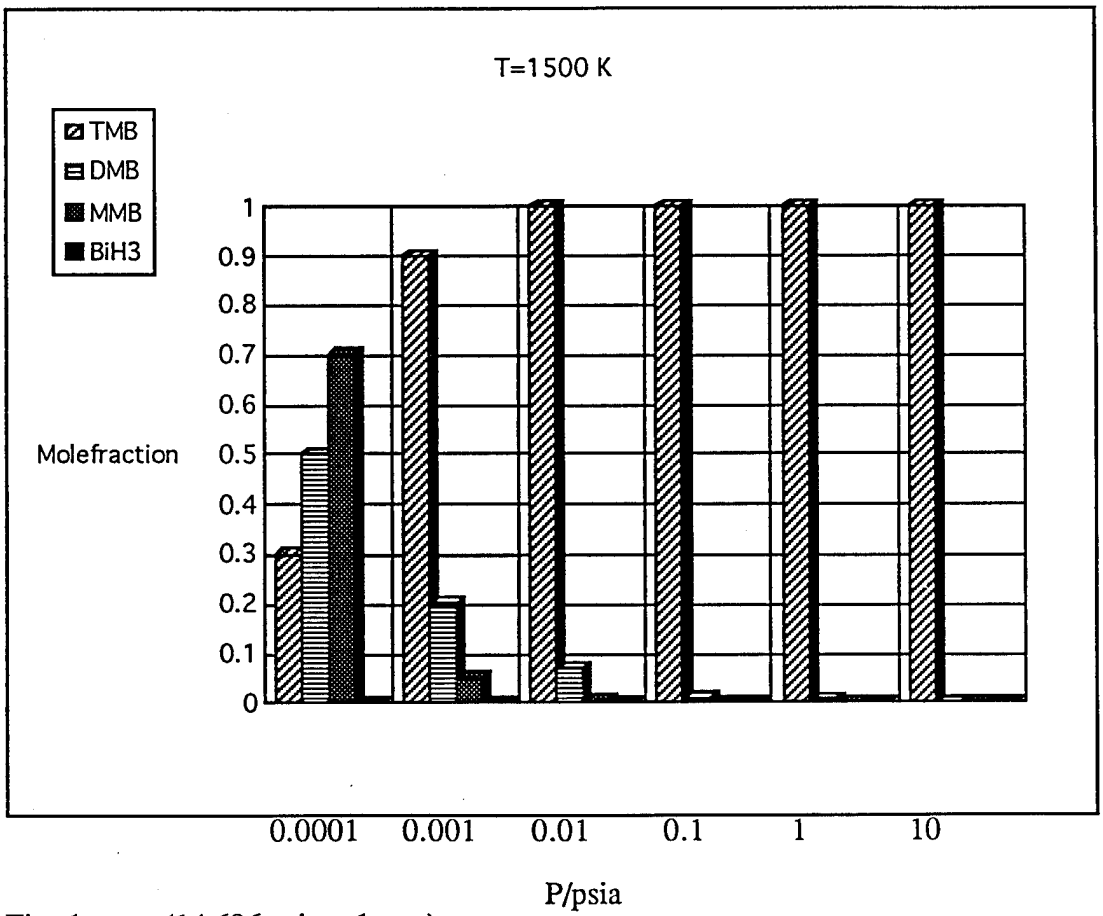

Fig. 1 (14.696 psia = 1 atm)

This study is divided into two main parts. The first section illustrates the behavior of pure TMB under different pressures and temperatures. After this combustor conditions favorable to CH_3 reduction and Bi production are discussed. In the second section thermochemical data for combustor compounds are presented for 298 K and 3800 K. Heats of reaction are given for likely combustor reactions at both temperatures. Finally TMB concentrations to be used in the combustor are given on the basis of previous shock tube experiments and conclusions reached here.

1) TMB dissociation as a function of pressure and temperature

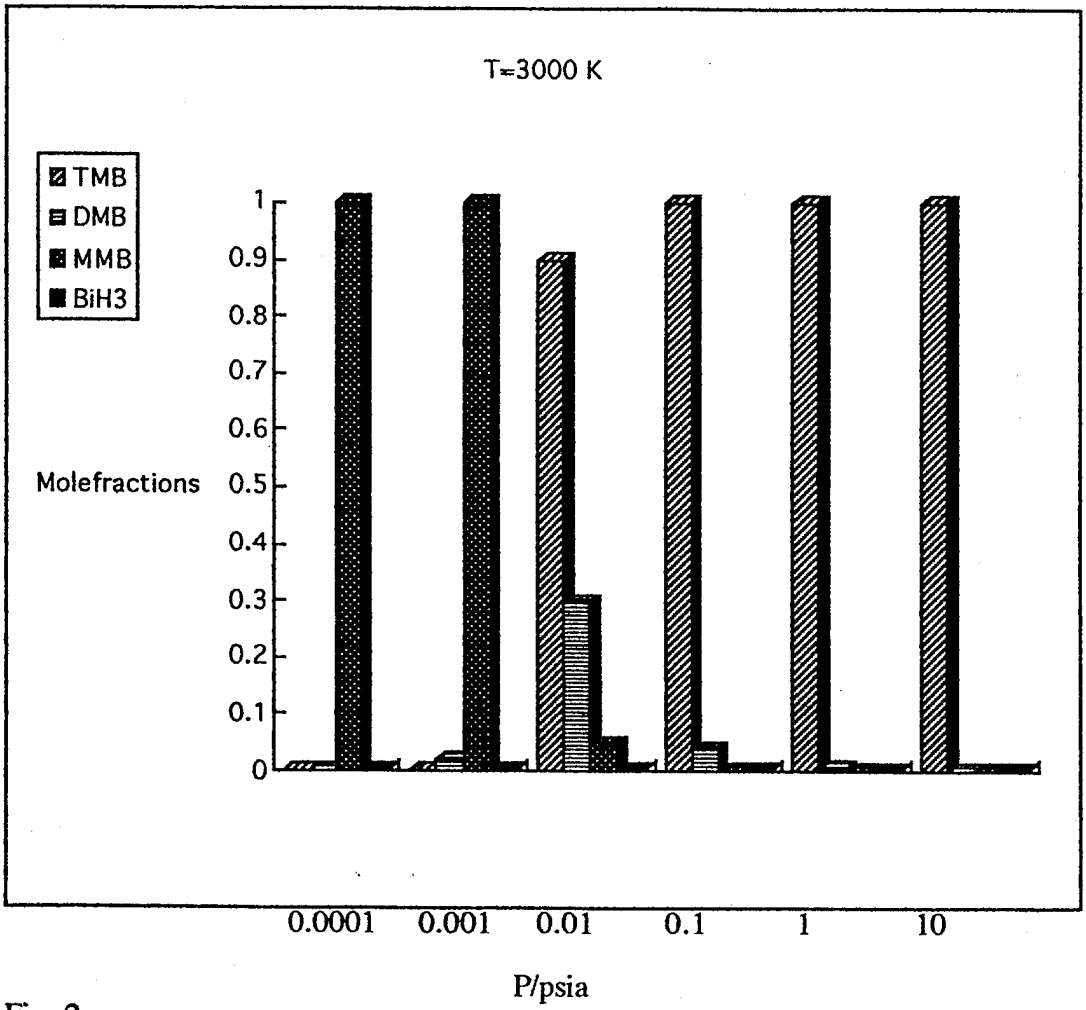

Fig. 2

Collisional stabilization of $Bi(CH_3)_3$ (TMB) at higher pressures is responsible for low Bi atom yields even at high temperatures. As can be seen in Fig. 1 even a 0.001 psia most of the TMB is undissociated.[2] The picture at 3000 K does not change significantly as illustrated in Fig. 2.[2]

The rate with which TMB dissociates as a function of temperature in a reactor at a presssure of 30 psia is shown in Fig. 3.[3] It is clear from this figure that temperatures well in access 1000 K have to be used to get reasonably fast dissocation rates.[3]

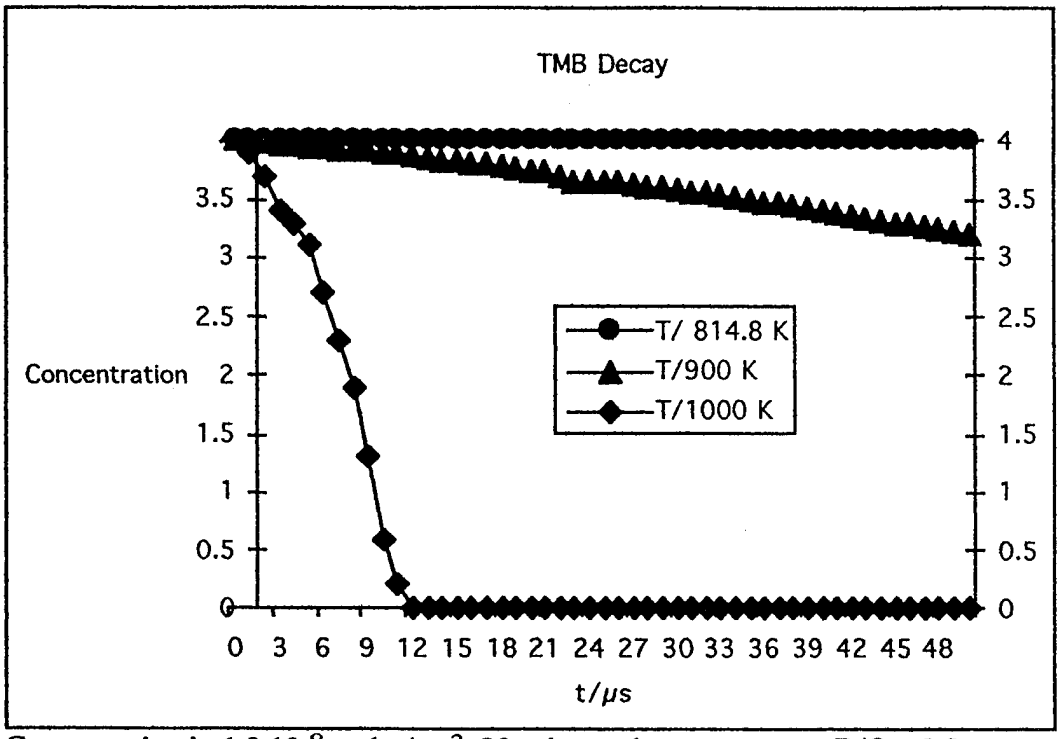

Concentration in 1.0 10^{-8} moles/cm^3, 30 psia combustor pressure, D/O = 3.8

Fig. 3

According to literature the slowest step in TMB dissociation is the first dissociation step into DMB and CH_3.[3] The dissociation of MMB is the fastest on the way to Bi + 3 CH_3.[3]

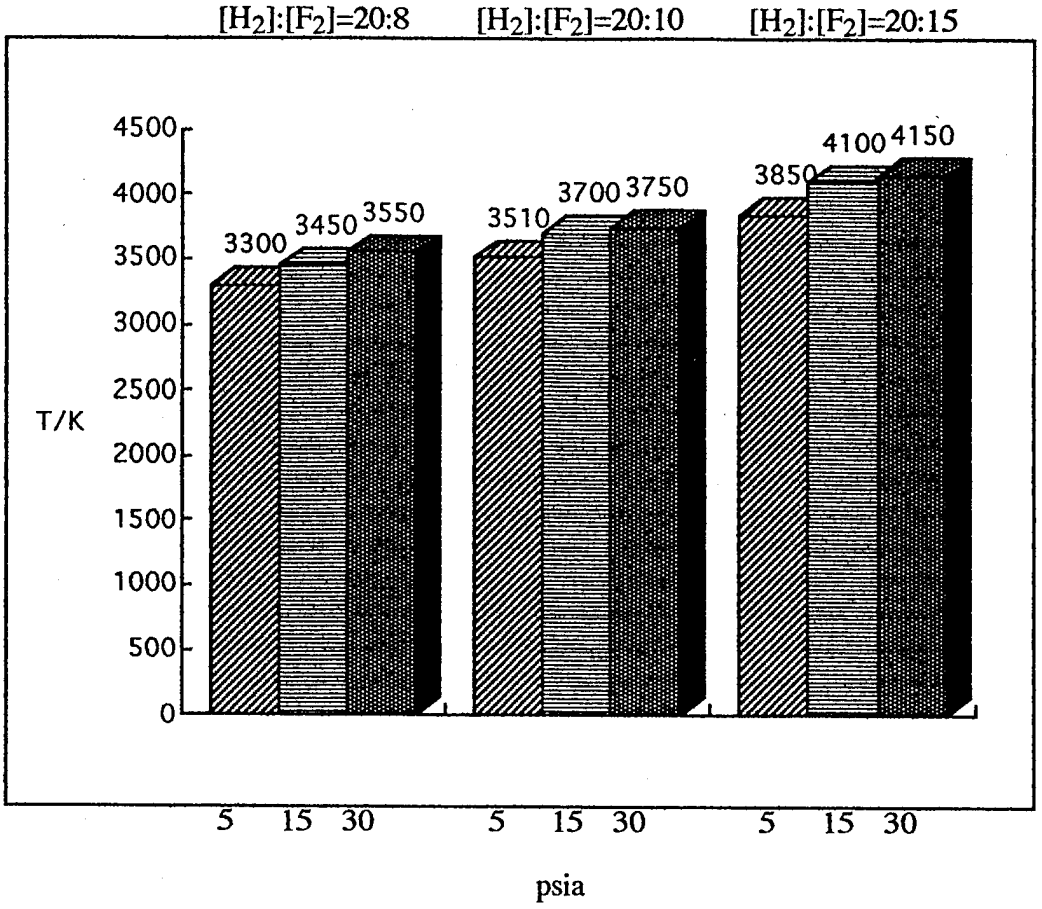

Fig. 4

Appropriately high temperatures for fast TMB dissociation and large H atom concentrations are achieved with $[H_2]$:$[F_2]$ ratios and pressures of ~ 20:15 and pressures between 10 - 15 psia.[4] Figure 4 shows the temperature reached is ~3800 K.[4] H atom molefractions as a function of fuel mixture $[H_2]$:$[F_2]$ and pressure are shown in Fig. 5.[4]

At 10 psia and a mixture of $[H_2]$:$[F_2]$:[TMB] = 20:12:0.4 temperatures of 3500 -3800 K are achieved, see Fig. 6.[2] The conditions given for the most desirable $[H_2]$:$[F_2]$ ratios and pressures are not changed significantly by the addition of TMB to the reaction mixture. The mole fraction of added TMB is small. Calculations performed under these conditions show that Bi is ejected from the combustor as a molecular complex rather than as atomic Bi.[2] The likely end product under H atom rich conditions are hydrides such as BiH_3.[2]

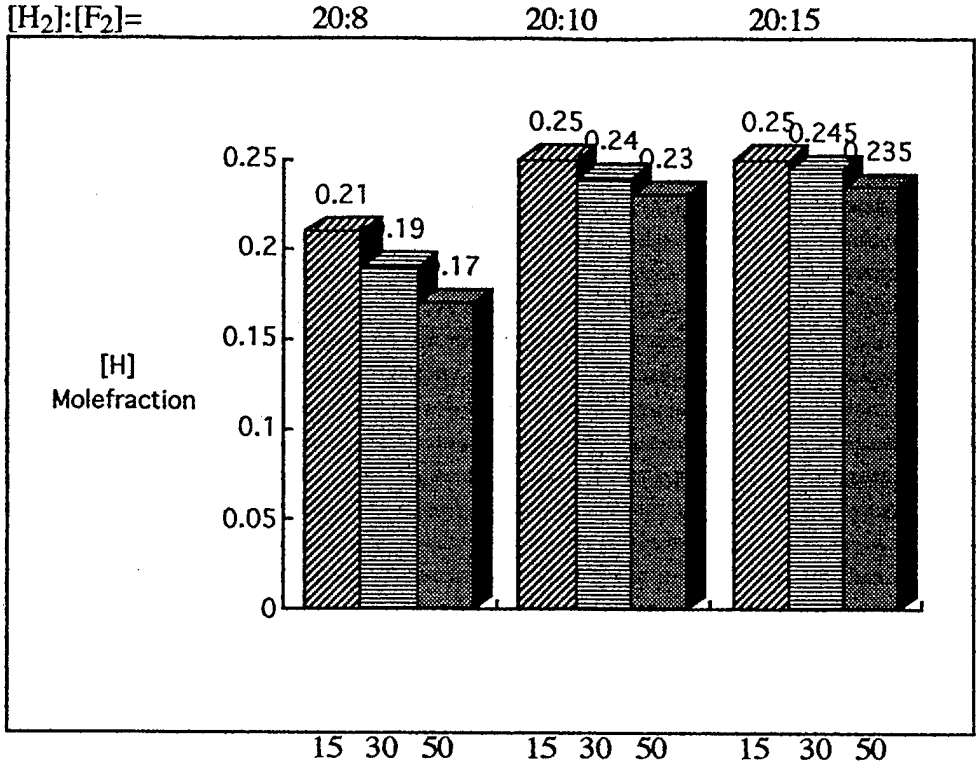

Fig. 5

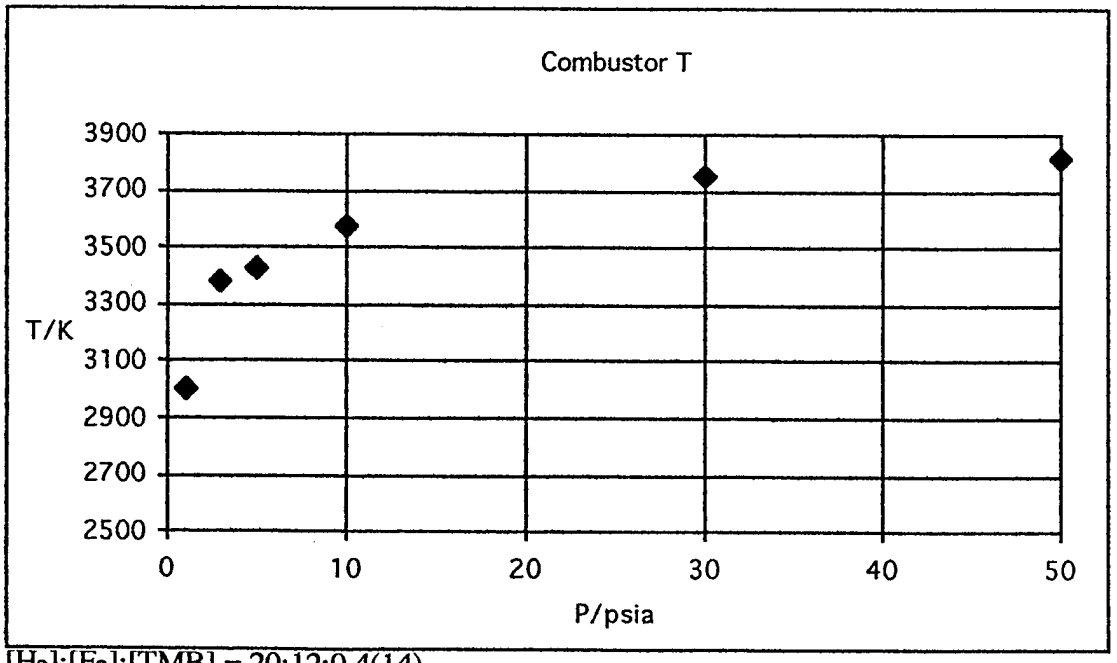

$[H_2]:[F_2]:[TMB] = 20:12:0.4(14)$

Fig. 6

The tables, which were used to create the figures in chapter 1 can be found in Appendix A.

2) Thermodynamical combustor properties

Heats of formation for 298 K and 3800 K are given in Table 8 and 9 in Appendix B.[1,5,7] Unfortunately the thermodynamical data set for BiH_X is incomplete. The value for the heat of formation of Bi(g) changed from 44.o to 50.1 kcal/mol. All heats of reaction are calculated with the new value of 50.1 kcal/mol. Pressure dependent Gibbs energies were calculated from 1 to 100 atm according to

$$\Delta G_f(p_f) = \Delta G_f(p_i) + n \bullet R \bullet T \bullet \ln(p_f/p_i)$$

with p_f = final pressure, p_i = initial pressure, R = 8.315 J/mol • K, T = 3800 K and n = 1 mol/cm^3. This formula has to be considered a first order approximation, since the real behavior of the gases in question is not taken into account. The result of the calculation can be found in Table 10.

Heats of reaction and Gibbs energies for the most likely combustor reactions are given in Table 11 for 298 and 3800 K and as a function of pressure. Many of the reactions listed in Table 11 are likely to involve a third collision partner. The idea was not to present a complete set of reactions, but to look for trends in the decomposition of TMB, DMB and MMB, the formation of HF and the reaction of CH_X with H atoms. Previously performed thermodynamical calculations done on the system for $[H_2]$:$[F_2]$:[TMB] mixtures 20:12:0.4 support that under hydrogen rich conditions CH_X fragments react away to CH_4.[2] In addition, free F atoms react with excess hydrogen atoms to form HF, which is also a benign quencher.[6] As mentioned before Bi atoms under these conditions are unlikely compared the BiH_X formation.[2]

The Gibbs energy of reaction helps to assess if a reaction happens spontaneously or not, and is in addition to the heat of reaction a valuable source of information. The trends shown here agree with the studies mentioned above. While the formation of CH_X and HF is likely to happen spontaneously according to Fig. 7 and Table 11, the decomposition of TMB, DMB and MMB is not, see Fig. 8. This seems at first contradictory to the statement that Bi will leave the reactor most likely as BiH_X.[2] The contradiction is due to the fact that thermodynamical considerations alone cannot solve the problem.

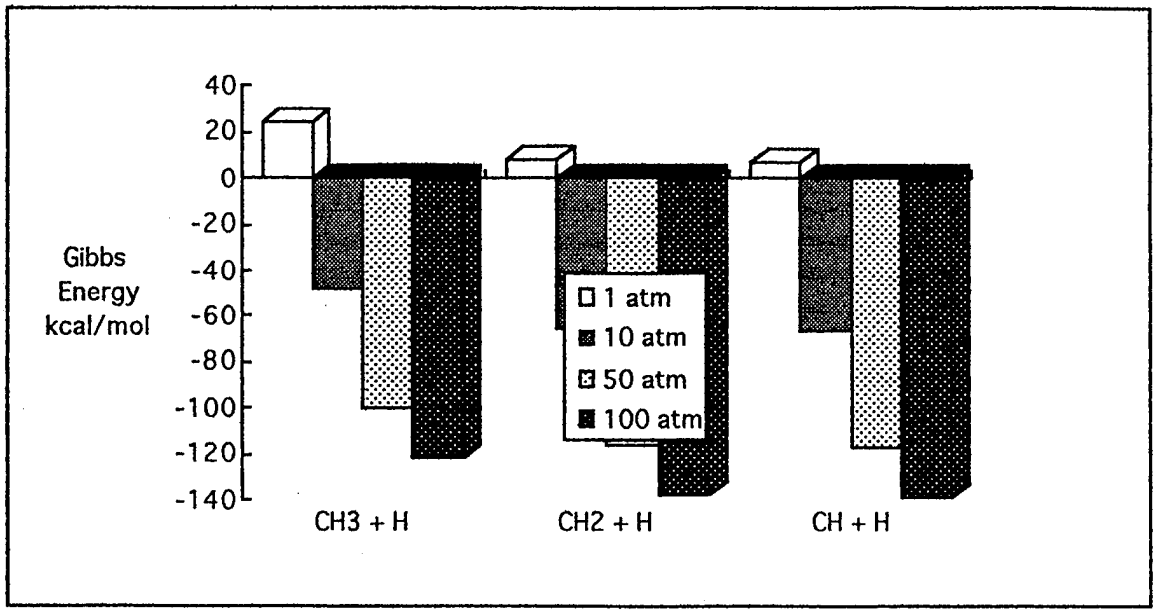
40
20
0
-20
-40
-60
-80
-100
-120
-140
Gibbs Energy kcal/mol
1 atm
10 atm
50 atm
100 atm
CH3 + H
CH2 + H
CH + H

Fig. 7

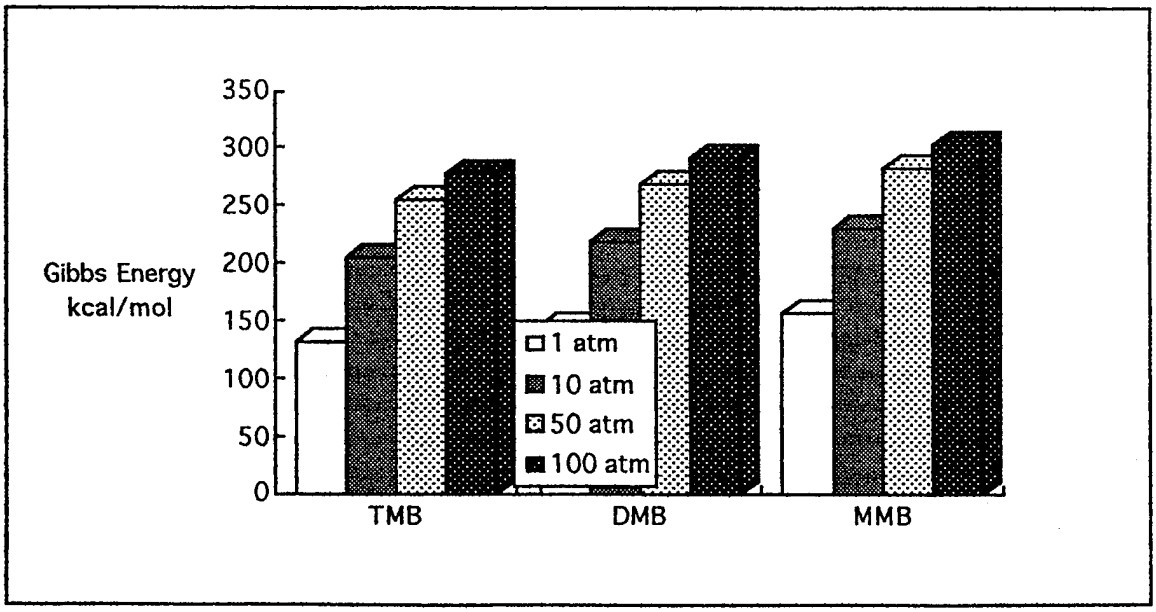
350
300
250
200
150
100
50
0
Gibbs Energy kcal/mol
1 atm
10 atm
50 atm
100 atm
TMB
DMB
MMB

Fig. 8

Calculations, which take dynamic effects into accout have been performed for systems very similar to the combustor problem discussed here.[2] On the basis of these studies it was possible to determine reasonable combustor conditions. Still, it is desirable to work with a reaction rate package specifically tailored to the combustor in question. A preliminary set of reactions is given in Table 12.

Results

It can be shown that TMB dissociates surprisingly slow. To achieve a reasonable dissociation rate elevated temperatures have to be used, which can be achieved with $[H_2]$:$[F_2]$ mixtures between 20:10 and 20:15.[4] When TMB is added to this system $[H_2]$:$[F_2]$:[TMB] Bi is set free from the combustor in form of BiH_x,[2] which is a good Bi source. Thermodynamical data and model calculations on combustors of the composition [He]:$[H_2]$:$[F_2]$:[TMB] = 1070:20:12:0.4 show that CH_x and F atoms are reacted to benign quenchers such as CH_4 and HF.[2,6] The discussion of the hydrogen atom concentration needed to reduce CH_x suffers from the fact that the exact mechanism for TMB decay is not known. In the worst case the H atom concentration is overstated and should be varied accordingly.

For the evaluation of feasible TMB concentrations previous shock tube studies are used with respect to NF(X) and NF(a) concentrations achieved under the applied conditions.[1] In previous shock tube experiments NF(a^1D) concentrations of $3 \cdot 10^{16}$ particles/cm^3 were achieved. TMB was added to the system in concentrations of $2 \cdot 10^{15}$ particles/cm^3 of which only $5 \cdot 10^{13}$ particles/cm^3 were converted to BiF(A).[1] This was in part due to slow TMB dissociation, but more to the fact that $2 \cdot 10^{15}$ particles/cm^3 introduced $6 \cdot 10^{15}$ moles/cm^3 CH_3 into the system. The improvements using the combustor for the same TMB concentration are (i) enhanced dissociation rate, (ii) production of BiH_x, (iii) HF and CH_4 as combustor end products. For an end temperature of ~3800 K a ratio of $[H_2]$:$[F_2]$ of 20:10 to 20:15 is needed. In order to react CH_x and F atoms away, the H_2 concentration is fairly high with $3 \cdot 10^{17}$ particles/cm^3, the F_2 atom concentration follows with ~ $1.5 \cdot 10^{17}$ particles/cm^3. To achieve a pressure of 10 psia, He has to be added up to $1.6 \cdot 10^{19}$ particles/cm^3. The addition of O_2 might be required to stabilize the fuel mixture suggested above.

Literature

1. D.J. Benard, J. Appl. Phys. **74**, 2900 (1993).
2. W.A. Duncan, SAIC Technical Report , "Advanced Short Wavelength Chemical Laser Analyses" (02/05/1991).
3. R. Malins, W. Smith, R. Acebal and R. Jones, SAIC Techincal Report, "Directed Energy Devices Technology Support" (09/03/1990).
4. R. Malins, W. Smith, R. Acebal, S. Taylor, J. Danserequ and W. Jones, SAIC Technical Report , "Bismuth Fluoride Short Wavelength Chemical" (12/18/1990).
5. JANAF Tables, J. Phys. Chem. Ref. Data **41**, (1985)
6. E. Quiñones, J. Habdas, D.W. Setser, J. Phys. Chem. **91**, 5155 (1987).
   J. Habdas, S. Wategaonkar, D.W. Setser, J. Phys. Chem. **91**, 451 (1987).
   Kang Yan Du, D.W. Setser, J. Phys. Chem. **94**, 2425 (1990).
7. W. Smith, R. Malins, R. Jones, R. Acebal, E. Schafer, W. Warren (PARC) and L. Schneider (PARC), SAIC Technical Report, "Directed Energy Technology Support, Bismuth Fluoride Analytical/Experimental Support" (01/31/1991).
8. D.L. Baulch, C.J. Cobos, R.A. Cox, C. Esser, P. Franc, Th. Just, J.A. Kerr, M.J. Pilling, J. Troe, R.W. Walker and J. Warnatz, J. Chem. Phys. Ref. Data 21, 418 (1992).

Appendix A

Table 1 Pressure Stabilization of TMB, DMB and MMB at T = 1500 K.[2]

P/psia	TMB	DMB	MMB	BiH_3
0.0001	0.3	0.5	0.7	0.001
0.001	0.9	0.2	0.05	0
0.01	1	0.07	0.003	0
0.1	1	0.01	0.0002	0
1	1	0.005	0	0
10	1	0.0009	0	0

Table 2 Pressure stabilization of TMB, DMB and MMB at T = 3800 K.[2]

P/psia	TMB	DMB	MMB	BiH_3
0.0001	0	0	1	0
0.001	0.0002	0.02	1	0
0.01	0.9	0.3	0.05	0
0.1	1	0.04	0.0008	0
1	1	0.006	0	0
10	1	0.0009	0	0

Table 3 Dissociation rates for TMB as a function of temperature.[3]

$t/\mu s$	T/ 815 K [TMB]	T/900 K [TMB]	T/1000 K [TMB]
0	4	4	4
1	4	3.99	3.9
2	4	3.98	3.7
3	4	3.97	3.4
4	4	3.96	3.3
5	4	3.95	3.1
6	3.95	3.94	2.7
7	3.95	3.93	2.3
8	3.95	3.92	1.9
9	3.95	0.91	1.3
10	4	3.9	0.6
11	4	3.89	0.2
12	4	3.87	0

t/μs	T/ 815 K [TMB]	T/900 K [TMB]	T/1000 K [TMB]
13	4	3.86	0
14	4	3.84	0
15	4	3.83	0
16	4	3.81	0
17	4	3.8	0
18	4	3.79	0
19	4	3.77	0
20	4	3.75	0
21	4	3.73	0
22	4	3.7	0
23	4	3.65	0
24	4	3.65	0
25	4	3.65	0
26	4	3.65	0
27	4	3.635	0
28	4	3.615	0
29	4	3.6	0
30	4	3.58	0
31	4	3.57	0
32	4	3.56	0
33	4	3.54	0
34	4	3.52	0
35	4	3.5	0
36	4	3.48	0
37	4	3.46	0
38	4	3.44	0
39	4	3.42	0
40	4	3.4	0
41	4	3.38	0
42	4	3.36	0
43	4	3.34	0
44	4	3.32	0
45	4	3.3	0
46	4	3.28	0
47	4	3.26	0
48	4	3.24	0
49	4	3.22	0
50	4	3.2	0

Table 4 Dissocation rates for TMB, DMB and MMB.[3]

Reaction	A/ cm^3 mol^{-1} s^{-1}	Ea/cal
TMB → DMB + CH_3	1.585 10^{14}	4.4 10^4
DMB → MMB + CH_3	1.585 10^{14}	3.86 10^4
MMB → Bi + CH_3	1.585 10^{14}	1.90 10^4

k in units of [cm^3/mol s], k = A exp(-Ea/RT)

Table 5 Temperatures achieved with different fuel mixtures [H_2]:[F_2] as a function of pressure.[4]

[H_2]:[F_2] = 20:8	T/K	[H_2]:[F_2] = 20:10	T/K	[H_2]:[F_2] = 20:15	T/K
5	3300	5	3510	5	3850
15	3450	15	3700	15	4050
30	3550	30	3750	30	4150

Table 6 [H_2] molefractions achieved with different fuel mixtures [H_2]:[F_2] as a function of pressure.[4]

[H_2]:[F_2] = 20:8	[H_2]	[H_2]:[F_2] = 20:10	[H_2]	[H_2]:[F_2] = 20:15	[H_2]
5	0.21	5	0.25	5	0.25
15	0.19	15	0.24	15	0.245
30	0.17	30	0.23	30	0.235

Table 7 Temperatures reached when TMB is added to the fuel mixture.[2]

P/psia	T/K
1	3000
3	3380
5	3425
10	3580
30	3750
50	3820

Appendix B

Table 8 P = 1 atm

Species	T = 298 K cp cal/mol K	T = 298 K ΔH_f kcal/mol	T = 298 K ΔG_f kcal.mol	T = 3800 K cp cal/mol K	T = 3800 K ΔH_f kcal/mol	T = 3800 K ΔG_f kcal/mol
Bi(g)	5.0	44.0 (50.1)	32.5	5.8	68.2	-206.0
Bi_2	NC	40.1	NC	NC	NC	NC
BiH	NC	29.4	NC	NC	NC	NC
BiH_2	NC	14.8	NC	NC	NC	NC
BiH_3	NC	-0.2	NC	NC	NC	NC
BiF	8.2	0	-21.8	10.8	-34.2	-332.8
BiF_2	12.3	-44.2	-68.1	14.3	-4.3	-431.5
BiF_3	15.4	-87.5	-112.1	20.3	-19.2	-516.4
$BiCH_3$	10.0	70.5	48.6	24.9	144.7	-308.6
$Bi(CH_3)_2$	15.5	97.1	72.6	47.7	237.5	-398.7
$Bi(CH_3)_3$	21.5	123.7	97.7	70.6	330.5	-474.8
CH	7.0	142.1	134.2	10.0	139.5	42.3
CH_2	8.3	92.4	88.3	13.9	87.4	48.5
CH_3	9.3	34.9	35.4	19.1	30.1	55.7
CH_4	8.5	-17.9	-12.2	24.8	-22.0	79.3
CH_2F_2	10.3	-107.8	-101.2	25.2	-109.4	-7.4
CH_3F	9.0	-56.1	-50.3	25.0	-59.2	38.3
HF	7.0	-65.2	-65.7	8.9	-66.9	-67.7
H	5.0	52.2	48.6	5.0	55.3	-0.76
F	5.4	19.0	14.9	5.0	21.1	-38.7

Table 9 T = 3800 K, ΔG_f/kcal mol^{-1}

Species	P = 1 atm	P = 10 atm	P = 50 atm	P = 100 atm
Bi(g)	-206.0	-133.2	-82.4	-60.5
Bi_2	NC	NC	NC	NC
BiH	NC	NC	NC	NC
BiH_2	NC	NC	NC	NC
BiH_3	NC	NC	NC	NC
BiF	-332.8	-260.0	-209.2	-187.3
BiF_2	-431.5	-358.7	-307.9	-286.0
BiF_3	-516.4	-443.6	-329.8	-370.9
$BiCH_3$	-308.6	-235.8	-185.0	-163.1
$Bi(CH_3)_2$	-398.7	-325.9	-275.1	-253.2
$Bi(CH_3)_3$	-474.8	-402.0	-351.2	-329.3
CH	42.3	115.1	165.9	187.8
CH_2	48.5	121.3	172.1	194.0
CH_3	55.7	128.5	179.3	201.2
CH_4	79.3	152.1	202.9	224.8
CH_2F_2	-7.4	65.4	116.2	138.1
CH_3F	38.3	111.1	161.9	183.8
HF	-67.7	5.1	55.9	77.8
H	-0.76	72.1	122.8	144.7
F	-38.7	34.1	84.9	106.8

Table 10

Reaction	T = 298 K ΔH_R kcal/mol	T = 298 K ΔG_R kcal/mol	T = 3800 K ΔH_R kcal/mol	T = 3800 K ΔG_R kcal/mol
$\Delta + H_2 \rightarrow 2\,H$	104.4	97.2	110.6	-1.5
$\Delta + F_2 \rightarrow 2\,F$	38.0	29.8	42.2	-77.4
$\Delta + TMB \rightarrow DMB + CH_3$	8.3	10.3	-62.9	131.8
$\Delta + DMB \rightarrow MMB + CH_3$	8.3	11.4	-62.7	145.8
$\Delta + MMB \rightarrow Bi + CH_3$	14.5	19.3	-46.4	158.3
$H + F \rightarrow HF$	-136.8	-129.2	-143.3	-28.2
$H + F_2 \rightarrow HF + F$	-98.4	-99.4	-101.1	-105.6
$F + H_2 \rightarrow HF + H$	-32.0	-32.0	-32.7	-29.8
$H + HF \rightarrow H_2 + F$	32.0	32.0	32.7	29.8
$H + H + M \rightarrow H_2 + M$	-104.4	97.2	-110.6	-1.5
$F + F + M \rightarrow F_2 + M$	-38.0	29.8	-42.2	-77.4
$CH_3 + F \rightarrow CH_2 + HF$	-26.7	-23.6	-30.7	-36.2
$CH_3 + F \rightarrow CH_3F$	-110.0	-100.6	-110.4	21.3
$CH_2 + F \rightarrow CH + HF$	-34.5	-34.7	-35.9	-35.2
$CH_4 + F \rightarrow CH_3 + HF$	-31.4	-33.0	-35.9	-52.6
$CH_2 + F + F \rightarrow CH_2F_2$	-238.2	-225.7	-219.3	21.5
$CH_3 + H \rightarrow CH_4$	-105.0	-96.4	-107.4	24.4
$CH_2 + H \rightarrow CH_3$	-109.7	-101.5	-112.6	8.0
$CH + H \rightarrow CH_2$	-101.3	-94.5	-107.4	7.0
$Bi + F \rightarrow BiF$	-69.1	-86.8	-123.5	-88.1
$BiF + F \rightarrow BiF_2$	-63.2	-61.2	8.8	-60.0
$BiF_2 + F \rightarrow BiF_3$	-62.3	-58.9	-36.0	-46.3
$Bi + F_2 \rightarrow BiF + F$	-31.1	-57.0	-81.3	-165.5
$Bi + F_2 \rightarrow BiF_2$	-94.3	-118.2	-72.5	-225.5
$Bi + 2F_2 \rightarrow BiF_3 + F$	-118.6	-147.3	-66.3	-349.1
$Bi + H \rightarrow BiH$	-72.9	NC	NC	NC
$BiH + H \rightarrow BiH_2$	-66.8	NC	NC	NC
$BiH_2 + H \rightarrow BiH_3$	-67.6	NC	NC	NC

$Bi + H_2 \rightarrow BiH + H$	31.5	NC	NC	NC
$Bi + H_2 \rightarrow BiH_2$	-35.3	NC	NC	NC
$Bi + 2H_2 \rightarrow BiH_3 + H$	1.9	NC	NC	NC
$BiF + H \rightarrow Bi + HF$	-67.7	-60.0	-19.8	60.0
$BiF_2 + H \rightarrow BiF + HF$	-73.2	-68.0	-152.1	31.8
$BiF_3 + H \rightarrow BiF_2 + HF$	-74.1	-70.2	-107.3	18.0
$BiH + F \rightarrow Bi + HF$	-63.5	NC	NC	NC
$BiH_2 + F \rightarrow BiH + HF$	-69.6	NC	NC	NC
$BiH_3 + F \rightarrow BiH_2 + HF$	-69.2	NC	NC	NC
$Bi(CH_3)_3 + F \rightarrow Bi(CH_3)_2CH_2 + HF$	NC	NC	NC	NC
$Bi(CH_3)_3 + F \rightarrow Bi(CH_3)_2 + CH_3F$	-101.7	NC	NC	NC
$Bi(s) \rightarrow Bi$	NC	NC	NC	NC
$Bi + Bi \rightarrow Bi_2$	60.1	NC	NC	NC
$Bi + CH_3 \rightarrow MMB$	-14.5	-19.3	46.4	-158.3

NC not calculated, no literature data available

Table 11 $T = 3800$ K, ΔG_R/kcal mol^{-1}

Reaction	P = 1 atm	P = 10 atm	P = 50 atm	P = 100 atm
$\Delta + H_2 \rightarrow 2\,H$	-1.5	144.2	245.6	289.4
$\Delta + F_2 \rightarrow 2\,F$	-77.4	68.2	169.8	213.6
$\Delta + TMB \rightarrow DMB + CH_3$	131.8	204.6	255.4	277.3
$\Delta + DMB \rightarrow MMB + CH_3$	145.8	218.6	269.4	291.3
$\Delta + MMB \rightarrow Bi + CH_3$	158.3	231.1	281.9	303.8
$H + F \rightarrow HF$	-28.2	-101.1	-151.8	-173.7
$H + F_2 \rightarrow HF + F$	-105.6	-32.9	18.0	39.9
$F + H_2 \rightarrow HF + H$	-29.8	43.1	93.8	115.7
$H + HF \rightarrow H_2 + F$	29.8	-43.1	-93.8	-117.7
$H + H + M \rightarrow H_2 + M$	-1.5	-144.2	-245.6	-289.4
$F + F + M \rightarrow F_2 + M$	-77.4	-68.2	-169.8	-213.6
$CH_3 + F \rightarrow CH_2 + HF$	-36.2	-36.2	-48.7	-36.2
$CH_3 + F \rightarrow CH_3F$	21.3	-51.5	-102.3	-124.2
$CH_2 + F \rightarrow CH + HF$	-35.2	-35.2	-35.2	-35.2
$CH_4 + F \rightarrow CH_3 + HF$	-52.6	-52.6	-52.6	-52.6
$CH_2 + F + F \rightarrow CH_2F_2$	21.5	-124.1	-137.1	-269.5
$CH_3 + H \rightarrow CH_4$	24.4	-48.5	-99.2	-121.1
$CH_2 + H \rightarrow CH_3$	8.0	-64.9	-115.6	-137.5
$CH + H \rightarrow CH_2$	7.0	-65.9	-116.6	-138.5
$Bi + F \rightarrow BiF$	-88.1	-160.9	-211.7	-233.6
$BiF + F \rightarrow BiF_2$	-60.0	-132.8	-183.6	-205.5
$BiF_2 + F \rightarrow BiF_3$	-46.3	-119.0	-169.8	-191.7
$Bi + F_2 \rightarrow BiF + F$	-165.5	-92.7	-41.9	-20.0
$Bi + F_2 \rightarrow BiF_2$	-225.5	-225.5	-225.5	-225.5
$Bi + 2F_2 \rightarrow BiF_3 + F$	-349.1	-276.3	-225.5	-203.6
$Bi + H \rightarrow BiH$	NC	NC	NC	NC
$BiH + H \rightarrow BiH_2$	NC	NC	NC	NC
$BiH_2 + H \rightarrow BiH_3$	NC	NC	NC	NC
$Bi + H_2 \rightarrow BiH + H$	NC	NC	NC	NC
$Bi + H_2 \rightarrow BiH_2$	NC	NC	NC	NC

$Bi + 2H_2 \rightarrow BiH_3 + H$	NC	NC	NC	NC
$BiF + H \rightarrow Bi + HF$	60.0	5.8	59.9	59.9
$BiF_2 + H \rightarrow BiF + HF$	31.8	85.7	31.8	31.8
$BiF_3 + H \rightarrow BiF_2 + HF$	18.0	17.9	18.0	18.0
$BiH + F \rightarrow Bi + HF$	NC	NC	NC	NC
$BiH_2 + F \rightarrow BiH + HF$	NC	NC	NC	NC
$BiH_3 + F \rightarrow BiH_2 + HF$	NC	NC	NC	NC
$Bi(CH_3)_3 + F \rightarrow Bi(CH_3)_2CH_2 + HF$	NC	NC	NC	NC
$Bi(CH_3)_3 + F \rightarrow Bi(CH_3)_2 + CH_3F$	NC	NC	NC	NC
$Bi(s) \rightarrow Bi$	NC	NC	NC	NC
$Bi + Bi \rightarrow Bi_2$	NC	NC	NC	NC
$Bi + CH_3 \rightarrow MMB$	-158.3	-231.1	-281.9	-303.8

Appendix C

Table 12 k / $cm^3\ mol^{-1}\ s^{-1}$, k / $cm^6\ mol^{-2}\ s^{-1}$

	T = 298 K		T = 3800 K	
Reaction	Forward	Backward	Forward	Backward
$He^* + H_2 \rightarrow 2\ H$	$3.5\ 10^{-3}$	$2.8\ 10^{15}$	$4.1\ 10^{13}$	$2.5\ 10^{14}$
$He^* + F_2 \rightarrow 2\ F$	$1.5\ 10^{8}$	$2.4\ 10^{13}$	$1.8\ 10^{13}$	$3.7\ 10^{12}$
$He^* + TMB \rightarrow DMB + CH_3$	$3.1\ 10^{6}$	NA	$4.0\ 10^{13}$	NA
$He^* + DMB \rightarrow MMB + CH_3$	$2.7\ 10^{7}$	NA	$4.7\ 10^{13}$	NA
$He^* + MMB \rightarrow Bi + CH_3$	$7.4\ 10^{10}$	NA	$8.7\ 10^{13}$	NA

$F + HF \rightarrow H + F_2$	$2.5\ 10^{-5}$	$4.6\ 10^{13}$	$1.9\ 10^{12}$	$1.1\ 10^{14}$
$H + F_2 \rightarrow HF + F$	$4.6\ 10^{13}$	$2.5\ 10^{-4}$	$1.1\ 10^{14}$	$1.9\ 10^{13}$
$F + H_2 \rightarrow HF + H$	$8.4\ 10^{13}$	$2.6\ 10^{8}$	$1.1\ 10^{14}$	$7.8\ 10^{13}$
$H + HF \rightarrow H_2 + F$	$2.5\ 10^{-5}$	$4.6\ 10^{13}$	$1.9\ 10^{12}$	$1.1\ 10^{14}$
$H + H + M \rightarrow H_2 + M$	$2.7\ 10^{15}$	$3.5\ 10^{-3}$	$2.4\ 10^{14}$	$4.1\ 10^{13}$
$F + F + M \rightarrow F_2 + M$	$2.4\ 10^{13}$	$1.5\ 10^{8}$	$3.7\ 10^{12}$	$1.8\ 10^{13}$
$CH_3 + F \rightarrow CH_2 + HF$	Reaction rates believed to be similar to that for the reaction of F atoms with CH_4.			
$CH_3 + F \rightarrow CH_3F$				
$CH_2 + F \rightarrow CH + HF$				
$CH_4 + F \rightarrow CH_3 + HF$	$4.8\ 10^{13}$	NA	NA	NA
$CH_2 + F + F \rightarrow CH_2F_2$	NA	NA	NA	NA
$CH_3 + H_2 \rightarrow CH_4 + H$	$5.1\ 10^{3}$	NA	$1.3\ 10^{13}$	NA
$CH + H_2 \rightarrow CH_2 + H$ $\rightarrow CH_3$	$3.9\ 10^{11}$	NA	NA	NA
$CH_4 + H \rightarrow CH_3 + H_2$	$4.5\ 10^{5}$	NA	$2.5\ 10^{14}$	NA
$CH_3 + H \rightarrow CH_4 + H_2$	505.6	NA	$8.1\ 10^{12}$	NA
$CH_2 + H \rightarrow CH + H_2$	$1.2\ 10^{14}$	NA	$7.6\ 10^{12}$	NA
$CH_3 + H + M \rightarrow CH_4$	NA	NA	NA	$1.2\ 10^{12}$
$CH_4 + H + M \rightarrow CH_3 + H + M$	NA	NA	NA	$6.3\ 10^{10}$
$Bi + F + M \rightarrow BiF + M$	$1.9\ 10^{18}$	18.8	$4.2\ 10^{13}$	$2.3\ 10^{12}$
$BiF + F + M \rightarrow BiF_2 + M$	$1.9\ 10^{19}$	24.0	$4.2\ 10^{14}$	$2.4\ 10^{12}$
$BiF_2 + F + M \rightarrow BiF_3 + M$	$1.9\ 10^{19}$	81.1	$4.2\ 10^{14}$	$7.3\ 10^{12}$
$Bi + F_2 \rightarrow BiF + F$	$3.9\ 10^{13}$	$2.1\ 10^{8}$	$1.4\ 10^{15}$	$1.1\ 10^{13}$
$Bi + F_2 \rightarrow BiF_2$	NA	NA	NA	NA
$Bi + 2F_2 \rightarrow BiF_3 + F$	NA	NA	NA	NA
$Bi + H + M \rightarrow BiH + M$	$1.9\ 10^{17}$	8.9	$4.2\ 10^{12}$	$5.8\ 10^{12}$
$BiH + H + M \rightarrow BiH_2 + M$	$1.9\ 10^{18}$	9.9	$4.2\ 10^{13}$	$6.4\ 10^{12}$
$BiH_2 + H + M \rightarrow BiH_3 + M$	$1.9\ 10^{18}$	10.2	$4.2\ 10^{13}$	$7.1\ 10^{12}$
$Bi + H_2 \rightarrow BiH + H$	$1.5\ 10^{6}$	$5.4\ 10^{12}$	$1.8\ 10^{13}$	$5.9\ 10^{13}$
$Bi + H_2 \rightarrow BiH_2$	NA	NA	NA	NA
$Bi + 2H_2 \rightarrow BiH_3 + H$	NA	NA	NA	NA

$BiF + H \rightarrow Bi + HF$	NA	NA	NA	NA
$BiF_2 + H \rightarrow BiF + HF$	NA	NA	NA	NA
$BiF_3 + H \rightarrow BiF_2 + HF$	NA	NA	NA	NA
$BiH + F \rightarrow Bi + HF$	NA	NA	NA	NA
$BiH_2 + F \rightarrow BiH + HF$	NA	NA	NA	NA
$BiH_3 + F \rightarrow BiH_2 + HF$	NA	NA	NA	NA
$Bi(CH_3)_3 + F \rightarrow Bi(CH_3)_2CH_2 + HF$	$5.1\ 10^{12}$	NA	$2.6\ 10^{13}$	NA
$Bi(CH_3)_3 + F \rightarrow Bi(CH_3)_2 + CH_3F$	NA	NA	NA	NA
$Bi(s) \rightarrow Bi$	NA	NA	NA	NA
$Bi + Bi \rightarrow Bi_2$	NA	NA	NA	NA

H + wall → products	probably slow compared to Bi + wall
F + wall → products	probably slow compared to Bi + wall
Bi + wall → products	NA
CH_3 + wall → products	probably slow compared to Bi + wall
CH_2+ wall → products	probably slow compared to Bi + wall
CH + wall → products	probably slow compared to Bi + wall
BiH_3 + wall → products	NA
BiH_2 + wall → products	NA
BiH + wall → products	NA
BiF_3 + wall → products	NA
BiF_2 + wall → products	NA

BiF + wall → products	NA
TMB + wall → products	NA
DMB + wall → products	NA
MMB + wall → products	NA

NA no literature data available